

UNITED STATES DEPARTMENT OF THE INTERIOR  
GEOLOGICAL SURVEY

An evaluation of potential  
volcanic hazards at the Radioactive  
Waste Management Complex,  
Idaho National Engineering Laboratory, Idaho

by

Mel A. Kuntz

G. Brent Dalrymple

Duane E. Champion

David J. Doherty

Open File Report 80-388

1980

## Table of Contents

---

	Page
Abstract.....	1
Introduction.....	2
Purpose .....	2
Location and physiography of the RWMC site.....	2
Previous studies.....	4
Rationale and methods of study.....	8
Stratigraphy and petrography.....	10
General stratigraphic relations.....	10
General petrographic relations.....	12
Petrography and stratigraphy of lava flows.....	14
Group A.....	14
Flow 1.....	14
Group B.....	16
Flow 2.....	16
Flow 3.....	17
Flow 4.....	18
Group C.....	19
Flow 5.....	19
Flow 6.....	21
Flow 7.....	22
Group D.....	25
Flow 8.....	25

Table of Contents (Cont.)

---

	Page
Stratigraphy and petrography (Cont.)	
Petrography of lava flows (Cont.)	
Group E.....	26
Flow 9.....	26
Group F.....	28
Flow 10.....	28
Flow 11.....	30
Group G.....	31
Flow 12.....	32
Flow 13.....	33
Correlation of flows with source vents.....	33
K-Ar Dating .....	34
Analytical techniques.....	34
Results .....	42
Paleomagnetism.....	46
Analytical techniques.....	46
Results .....	48
Age and frequency of eruption of lava flows.....	54
Application of data to evaluation of volcanic hazards at the	
Radioactive Waste Management Complex.....	58
Acknowledgments.....	60
References cited.....	61

Illustrations

---

	Page
Figure 1. Map showing location of Radioactive Waste Management Complex, Idaho National Engineering Laboratory, Arco, Howe, Big Lost River, Big Lost River Sinks, Arco volcanic rift zone, Big Southern Butte, Cedar Butte, faults, graben and vents.....	3
2. Map of the Radioactive Waste Management Complex showing location of wells.....	5
3. Stratigraphy of lava flows in cored drill holes at the Radioactive Waste Management Complex, Idaho National Engineering Laboratory, Idaho.....	9
4. Cumulative curves showing the difference between replicate mass analyses on the same extraction gas.....	41
5. Theoretical error curve for K-Ar ages as a function of the percentage of radiogenic $^{40}\text{Ar}$ in the sample gas. Based on the error formula of Cox and Dalrymple (1967).....	44
6. Values of magnetic inclination plotted as a function of depth below the surface for drill cores 94, 77-1, and 76-6.....	49

Tables

---

	Page
Table 1. Potassium-argon age data for samples of basalt from drill holes at the Radioactive Waste Management Complex, Idaho National Engineering Laboratory.....	37,38,39,40
2. Mean flow ages for data in Table 1.....	43
3. Mean magnetic inclination values for lava flows in three cores from the Radioactive Waste Management Complex, Idaho National Engineering Laboratory, Idaho.....	51
4. Summary of lava flow frequency represented in drill cores from the Radioactive Waste Management Complex, Idaho National Engineering Laboratory, Idaho.....	56

## ABSTRACT

The chief volcanic hazard at the Radioactive Waste Management Complex at the Idaho National Engineering Laboratory, located between Arco and Idaho Falls in southeastern Idaho, is potential inundation of the site by pahoehoe basalt lava flows erupted from vents within the surrounding topographic basin. Stratigraphic, radiometric, and paleomagnetic studies show that the waste storage site has been inundated by at least 18 lava flows and flow units erupted from 7 or more separate source vents in the last 500,000 years. The lava flows and flow units were erupted in seven groups of one to as many as five flows each.

Our data show that each eruption event that formed such a group lasted less than 200 years, that the group-forming eruption events were separated by long intervals during which no lava flows entered the area, and that the eruptions were episodic rather than periodic. The radiometric data suggest that groups of flows can be assigned to three major eruption episodes that occurred about 450,000, 225,000, and 75,000 years ago. The radiometric data also suggest that intervals between major eruption episodes are as long as 225,000 years and as short as 150,000 years, and that the last eruption episode that produced lava flows that covered the storage site occurred about 75,000 years ago. Approximately one in every five volcanic eruptions within the topographic basin in about the last 200,000 years has produced lava flows that eventually reached the Radioactive Waste Management Complex site.

## INTRODUCTION

### Purpose

This report describes the potential volcanic hazards and the recurrence intervals of volcanic events that have affected the site of the Radioactive Waste Management Complex (RWMC) at the Idaho National Engineering Laboratory (INEL), located between Arco and Idaho Falls in southeastern Idaho. The RWMC is used for the temporary storage of radioactive waste materials in both near-surface burial and above-ground storage. The U.S. Geological Survey began the study of volcanic hazards at INEL in 1974. A preliminary report (Kuntz, 1978b) on the geology of the area surrounding the RWMC qualitatively assessed potential volcanic hazards at the RWMC. Volcanic recurrence intervals were evaluated superficially in that report, owing to a lack at that time of radiometric data on lava flows that had buried the site in the past. Consequently, the U.S. Geological Survey proposed to the U.S. Department of Energy to study the petrology and stratigraphy of lava flows sampled by existing drill cores at the RWMC site and further proposed to date the flows by radiometric and paleomagnetic methods so as to estimate more quantitatively the volcanic recurrence intervals.

This report summarizes results of that investigation, incorporates results of the previous study by Kuntz (1978b), and evaluates volcanic recurrence intervals and volcanic hazards at the RWMC.

### Location and physiography of the RWMC site

The RWMC occupies 144 acres in the southwestern part of the INEL about 35 km southeast of Arco, Idaho (fig. 1). The burial site is in a shallow valley bordered on the north, west, and south by low hills and ridges of basalt. The central lower parts of the valley, where the RWMC is located, are veneered by eolian and alluvial sand, silt, and clay (Barraclough and others, 1976).

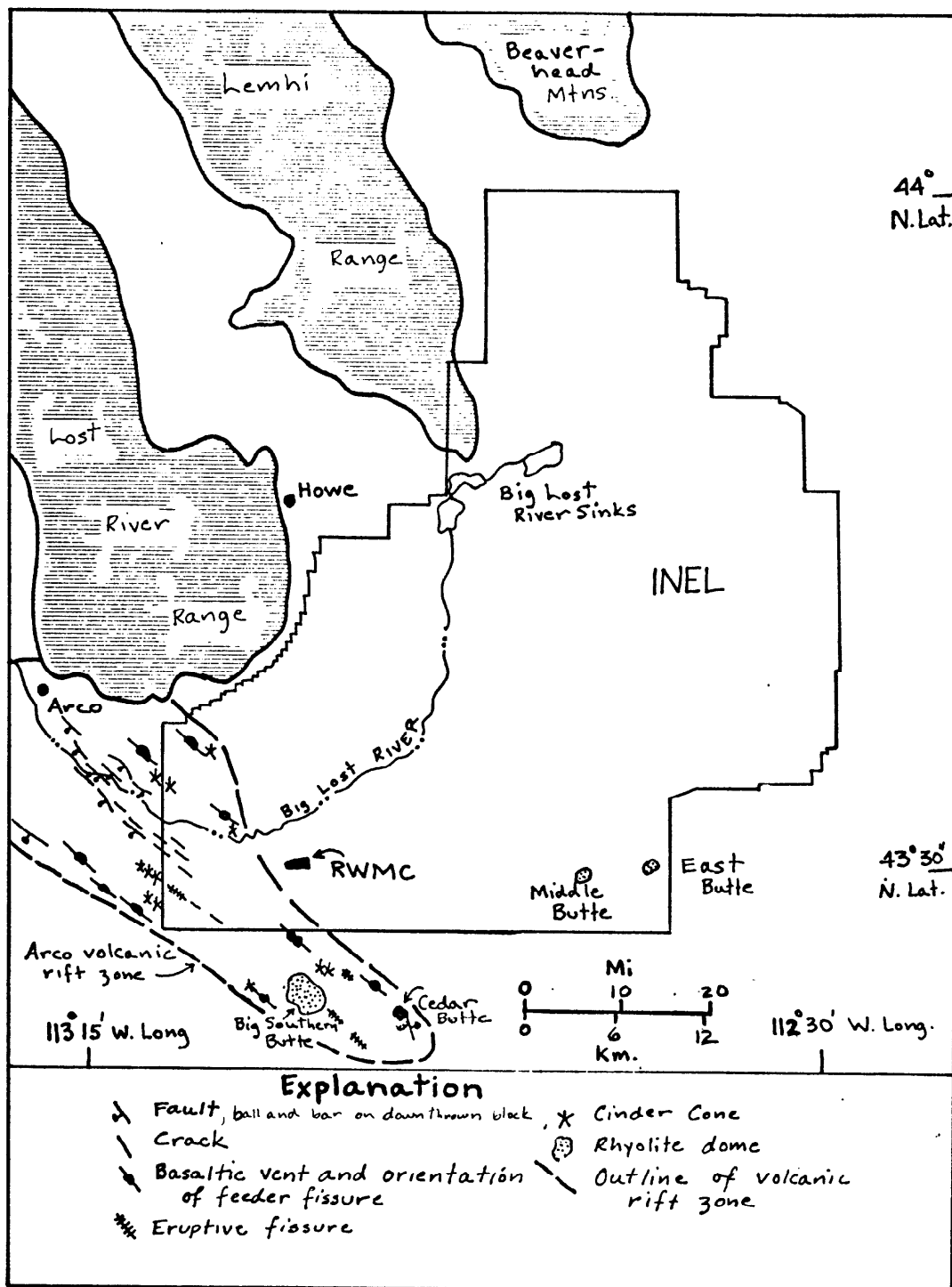


Figure 1.—Map showing location of Radioactive Waste Management Complex (RWMC), Idaho National Engineering Laboratory (INEL), and geographic locations referred to in the text. Geologic features from Kuntz (1978a).

The RWMC lies in a topographic depression--the floodplain of the Big Lost River. The RWMC is separated from the riverbed of the Big Lost River, about 2 km to the north, by a ridge formed by the distal end of a basalt lava flow. The configuration of the flow ridge suggests that it filled an old channel of the Big Lost River (Kuntz, 1978b).

#### Previous studies

Since 1970, the potential subsurface migration of radionuclides has been monitored at the RWMC. Monitoring by the U.S. Geological Survey (U.S.G.S.) (Barracough and others, 1976) has been followed up by studies by the Department of Energy (Burgus and Maestas, 1976; Humphrey and Tingey, 1978). In connection with the U.S.G.S. study, 10 monitoring wells were drilled in and near the RWMC. Four wells (well numbers 87, 88, 89, 90), located 275 m to 500 m outside the boundaries of the RWMC, were drilled by cable-tools to depths ranging from 191 to 197 m below the surface (fig. 2), and lithologic logs (Barracough and others, 1976) were prepared from cuttings. Six wells (well numbers 91, 92, 93, 94, 95, 96) located within the boundaries of the RWMC were cored and reached depths ranging from 80 m to 92.1 m below the surface (fig. 2).

Three of the six drill cores (well numbers 93A, 94, 95) were logged and sampled for this study.

Conclusions reached from observations made on the 10 wells are as follows (Barracough and others, 1976):

1. The RWMC is underlain by groups of basalt lava flows separated by sedimentary interbeds.
2. Two main sedimentary interbeds are at depths of approximately 34 m and 73 m; a surficial layer of sediment is on top of bedrock.

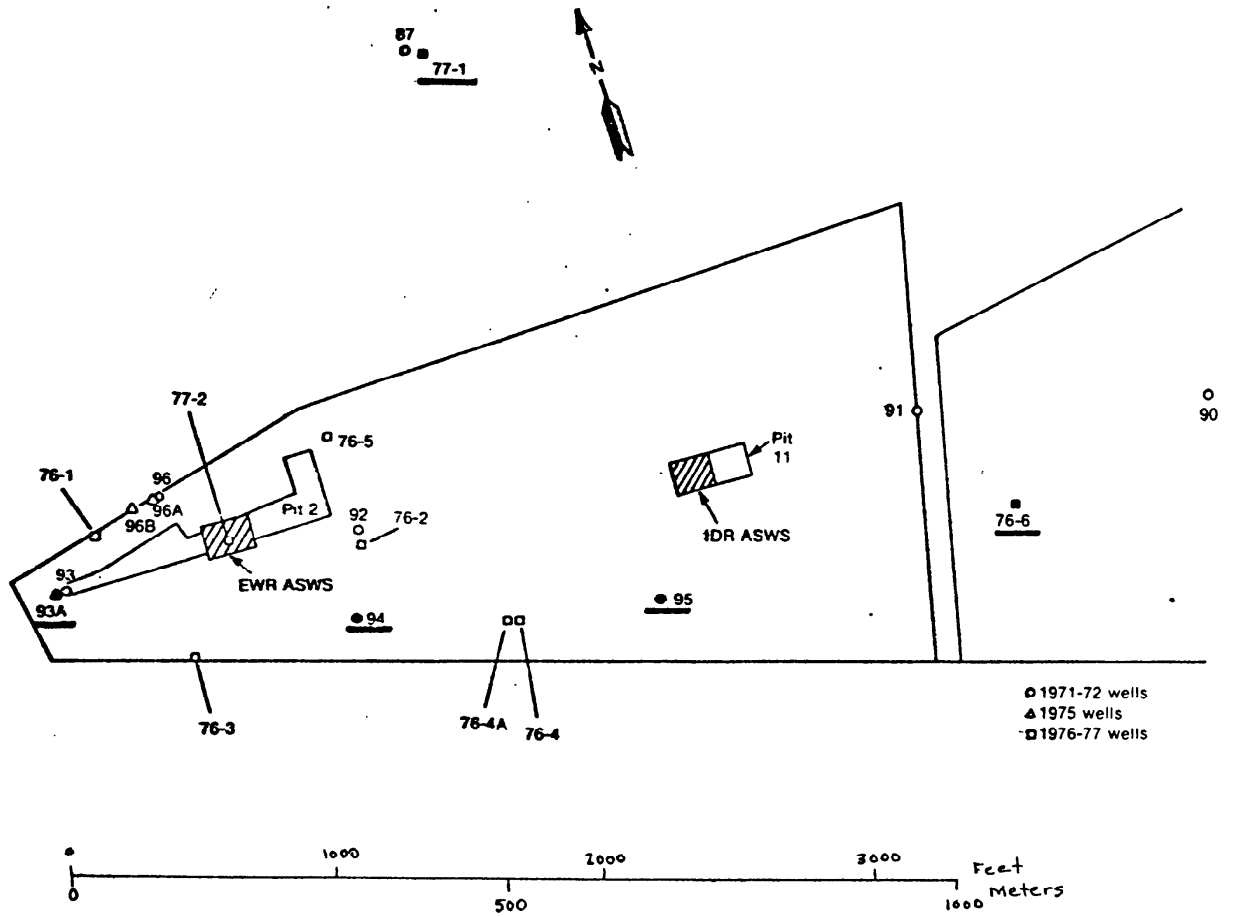


Figure 2.--Map of the Radioactive Waste Management Complex (RWMC) at the Idaho National Engineering Laboratory (INEL), showing location of wells. Underlined well numbers show locations of wells studied in this report. Map from Humphrey and Tingey (1978).

3. In the RWMC and immediate surrounding valley, the surficial layer of sediment is 1 to 7.6 m thick; the 33 m interbed is present in all 10 wells, and ranges from 0.3 m to 7.9 m in thickness. The 73 m interbed was also identified in all 10 wells, and its thickness ranges from 1.2 m to 9.8 m. Additional sedimentary interbeds were noted in some (but not all) wells that penetrate deeper than the 73 m interbed. Sediment layers that may extend beneath the entire area of the RWMC occur at about 111 m and at 165 m.
4. The sediments consist of unconsolidated clay, silt, sand, and gravel. They contain pebbles and granules of quartz, quartzite, metamorphic rocks, and siliceous volcanic rocks characteristic of terranes in the mountainous areas north of the Snake River Plain. The lithologies of the pebbles thus suggest that the sediments were deposited chiefly by streams draining these mountainous areas. The present Big Lost River drains the Lost River Valley between the Pioneer and Lost River Mountain Ranges and enters the Snake River Plain near Arco (fig. 1).

The Big Lost River flows southeastward from Arco about 25 km. It then turns northeast to north and flows about 40 km into a closed basin called the Big Lost River Sinks near the town of Howe (fig. 1). The RWMC is about 4 km from the present course of the Big Lost River. The river probably formerly traversed the present site of the RWMC and deposited much of the interbedded sediments between lava flows.

Ten additional cored holes (well numbers 93A, 96B, 76-1, 76-2, 76-3, 76-4, 76-4A, 76-5, 76-6, 77-1; see fig. 2) have been drilled in and near the RWMC since 1972 to aid in the continuing study of subsurface migration of radionuclides from the burial site (Burgus and Maestas, 1976; Humphrey and

Tingey, 1978). Cores from two of these (well numbers 93A, 77-1) were studied by us. The additional wells penetrated as deep as 183 m, and they yielded further information about deeper lava flows and interbeds below the 73 m interbed. The lithology and geochemistry of all drill cores, with particular reference to the sedimentary interbeds, are under investigation by Craig Rightmire, formerly of the U.S. Geological Survey, but no results or conclusions from his studies have yet been published.

Kuntz (1978a,b) mapped and described the geology of the Arco-Big Southern Butte area to establish a framework for assessing potential volcanic hazards for the RWMC and other waste storage and reactor facilities at INEL. The Arco-Big Southern Butte area covers 1,700 km<sup>2</sup> roughly centered on the RWMC. The area includes the Arco volcanic rift zone, which extends southeast 50 km from Arco to about 10 km southeast of Big Southern Butte (fig. 1). The rift zone is the locus of extensional faults, graben, fissure-controlled basaltic volcanic vents, the two rhyolite domes that constitute Big Southern Butte, and a volcano at Cedar Butte that erupted lavas ranging in composition from ferrobasalt to ferrolatite (Fountain and Spear, 1979). The limited radiometric age data available in 1979 and geological field criteria suggested that nearly all basaltic vents in the Arco-Big Southern Butte area are younger than 700,000 years old.

Kuntz (1978b) noted that the RWMC lies in the lowest part of a broad topographic basin covering an area of about 825 km<sup>2</sup>. He also identified at least 47 volcanic vents that he determined to be less than about 200,000 years old within the topographic basin. He concluded that lava flows originating from vents within the topographic boundaries of the basin all had the potential of reaching the site of the RWMC. Because there is no evidence at the surface or in drill cores that the RWMC has been the site of a volcanic

vent, Kuntz concluded that the chief volcanic hazard for the RWMC is future inundation by lava flows erupted from distant and nearby source vents. His report also discussed volcanic hazard scenarios based on various kinds of possible future volcanic eruptions within the boundaries of the RWMC and on possible eruptions some distance from the RWMC but within the topographic basin.

#### Rationale and methods of study

The conclusion that the chief volcanic hazard for the RWMC is inundation by lava flows from vents outside the boundaries of the RWMC prompted us to study the stratigraphy and age of lava flows exposed in drill cores at the burial site. Not all eruptions within the topographic basin in the past produced lava flows that reached the RWMC site. Thus, we felt that a radiometric study of the flows in the drill cores would allow us to determine the mean occurrence time for inundation of the RWMC site by lava flows and to determine what percentage of eruptions within the topographic basin reached the RWMC site in the past.

Our study consisted of three parts: (1) field and laboratory study of cores to determine the number and stratigraphic relationships of lava flows and sedimentary interbeds beneath the RWMC and to attempt to correlate the flows with possible source vents, (2) K-Ar study of selected lava flows to determine their age and eruption frequency, and (3) paleomagnetic measurements of the inclination of the natural remanent magnetism (NRM) as an aid in correlating and dating the flows.

We selected 5 cored drill holes for careful logging and sampling (fig. 3). The logging involved hand sample identification and description of core material, location of tops and bottoms of flows and flow units, preparation of lithologic logs, and correlation of flows between drill

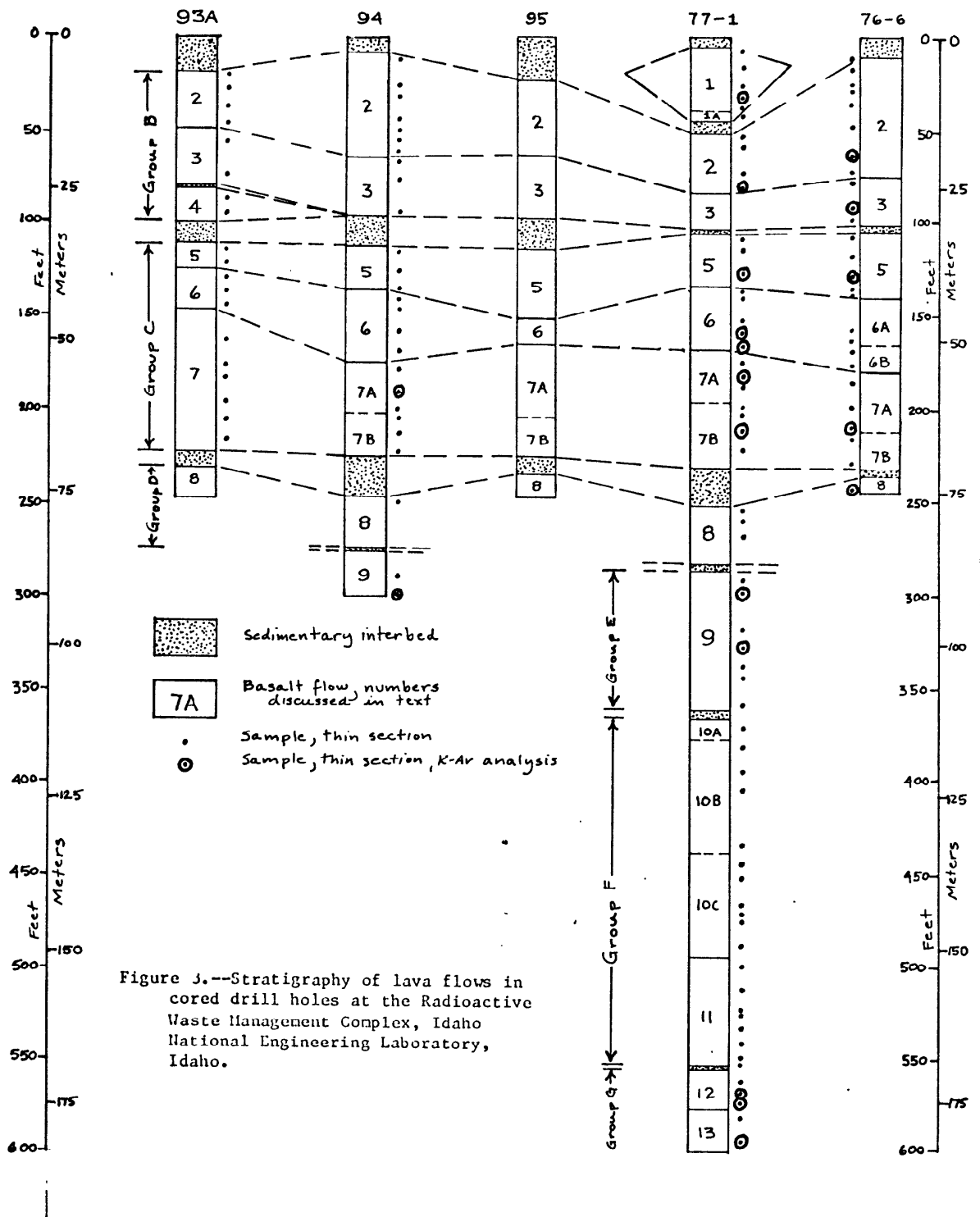


Figure J.--Stratigraphy of lava flows in cored drill holes at the Radioactive Waste Management Complex, Idaho National Engineering Laboratory, Idaho.

holes. We sampled flows at critical places for petrographic analyses, K-Ar analyses, and paleomagnetic measurements (fig. 3). We studied thin sections of lava flows from vents within the eruption basin to help correlate cores with possible source vents.

Thin sections were used to petrographically check the correlations based on prior megascopic observations of the core. The thin sections were also used to help choose samples for K-Ar analyses. The analytical techniques used in the K-Ar and the paleomagnetic studies are described in detail on later pages.

#### STRATIGRAPHY AND PETROGRAPHY

##### General stratigraphic relations

Core and thin-section studies show that the RWMC is underlain by groups of lava flows separated by sedimentary interbeds (fig. 3). A group of flows consists of one or more flows, each of which has an easily identifiable top and bottom surface. All flows within each group have similar petrographic characteristics, suggesting that the flows represent flow units erupted from the same source vent or flows erupted from several source vents that tapped the same magma source. Flow units within a group have clinkery, scoriaceous tops and bottoms, but they are not separated by sedimentary interbeds, with the exception of flows 3 and 4 in drill core 93A. We use the term "flow unit" here in its conventional sense to represent a separate sheet of lava that flows over earlier sheets erupted during the course of a single eruption. The absence of sedimentary interbeds between flow units suggests, but does not prove, that the flow units were emplaced within time intervals of perhaps days, weeks, months, or possibly a few years. The sedimentary interbeds may have formed during periods of volcanic quiescence lasting as long as hundreds or even thousands of years, when the upper surface of the topmost lava flow

was exposed and then covered by accumulations of eolian and alluvial sediments. Alternatively, flows may have dammed local drainage and floods may have deposited alluvial sediments on top of the flows during periods as short as a few months or years.

Lava flows and flow units observed in the drill cores typically consist of three gradational structural and textural units:

(1) A thin (typically <2 m thick) upper layer of fine-grained, vertically and horizontally jointed, vesicular and locally clinkery basalt forms the top of each flow or flow unit. Where the surface of a layer was intensely heated by the overlying flow, it is reddened by oxidation. The reddish color appears to be caused by oxidation of glassy matrix and olivine crystals and by a surface coating of reddish iron oxides and iron hydroxides on scoria fragments, in vesicles, and on fracture surfaces.

(2) A massive central layer consists of coarser grained, typically diktytaxitic lava that has prominent vertical columnar joints and has vesicles arranged in vertical pipes and horizontal layers. The thickness of the central layer ranges from several meters to as much as 20 m, depending on the total thickness of the flow. The central layer generally constitutes 75 percent or more of the total thickness of each flow.

(3) A thin (typically <1 m) basal layer, typically oxidized, consists of fine-grained scoriaceous blocks of basalt.

Flows in groups A, B, and C within the RWMC have been identified by the examination of cores and thin sections from 5 drill holes (well numbers 93A, 94, 95, 77-1, 76-6) that penetrated the 73-meter deep sedimentary interbed. The identity of flows in groups D, E, F, and G is based on examination of cores and thin sections from samples of drill core 77-1 only; thus, the

regional extent of these groups of flows is unknown. It is unknown whether the sedimentary interbeds separating these latter groups of flows have regional or local extent. However, the flows in groups D, E, F, and G are sufficiently distinct petrographically to indicate that they are separate packets of flows and flow units erupted either from different source vents or at significantly different times.

#### General petrographic relations

All flow units studied are very similar petrographically. All are tholeiitic olivine basalts that consist of olivine, plagioclase, clinopyroxene, ilmenite, magnetite, glass, and accessory apatite and zircon(?). Alteration, where present, consists of reddish films on fracture surfaces and crystal faces of olivine and, where severe, of an opaque coating on crystal faces. A carbonate mineral (calcite?) is ubiquitous as a coating on vesicle walls and also occurs, rarely, as an alteration of the matrix of porphyritic rocks.

Olivine occurs as phenocrysts and (or) as a constituent of the matrix. Phenocrysts are mostly equant in square, rectangular, wedge, and six-sided forms, but some are irregular. Nearly all phenocrysts contain small (<0.1 mm) square to irregular inclusions, either opaque (probably a spinel phase) or reddish-brown (chromite?). Nearly all thin sections contain glomeroporphyritic clots consisting of 2 to 15 crystals of olivine or intergrowths of olivine and plagioclase. Most olivine in the matrix of both inequigranular and equigranular rocks is subhedral to anhedral. In all flows optical properties suggest that the larger olivine crystals have chemical compositions ranging from Fo<sub>50</sub> to Fo<sub>90</sub>.

Plagioclase phenocrysts and smaller matrix crystals occur in most thin sections examined. They range in shape and size from lath-shaped crystals as

long as 4 mm with length-width ratios as high as 25:1 to crystals that are equant and nearly submicroscopic. Many thin sections contain aggregates of plagioclase laths arranged in irregular sheafs, bundles, crosses or X-shaped clusters. Glomeroporphyritic clots of plagioclase and olivine crystals are common. Most larger plagioclase crystals are normally zoned; maximum compositional variation between zones is 20 percent An. A few large, rectangular crystals have oscillatory zoning, again with compositional variation within the limits of 20 percent An. A few large crystals have exsolution patterns that suggest spinodal decomposition. Some crystals contain irregular-shaped blebs of included glass. Extinction angles indicate that nearly all the large crystals range in composition from An<sub>45</sub> to An<sub>72</sub>; and the average is about An<sub>65</sub>. Alkali feldspar was not observed in any thin sections.

Clinopyroxene occurs in nearly all thin sections examined as an anhedral phase of the matrix. Euhedral phenocrysts of clinopyroxene were lacking, but some rocks contain anhedral, ophitic crystals as large as 4 mm across. Small intergranular, anhedral crystals are interspersed between plagioclase laths in nearly all examined thin sections of the inequigranular rocks. Blade-like pyroxene crystals as long as 2 mm border the vesicle walls in a few thin sections in which most of the pyroxene is intergranular. Textures of the clinopyroxene range from ophitic to subophitic to intergranular, and any or all of these three textural types may appear in a single thin section. The clinopyroxenes are light tan in plane polarized light; they have very weak absorption colors and have optical properties that suggest a composition of augite.

Opaque minerals take two forms: (1) slender blades and needles probably ilmenite and (2) equant crystals with square, rectangular, or irregular shapes

(probably magnetite or titanomagnetite). The proportions, sizes, and shapes of these minerals are characteristic features that have been used to correlate flows between drill cores and to attempt to correlate flows with source vents. Ilmenite blades and needles have length-to-width ratios ranging from 3:1 to 30:1, and their sizes range from submicroscopic to crystals as much as 1.5 mm long. Magnetite-titanomagnetite crystals reach lengths of 1 mm. Both ilmenite and magnetite-titanomagnetite crystals are typically  $\leq$  0.5 mm long in most thin sections studied. Dispersed submicroscopic opaque particles render the matrix of the rock nearly opaque in a few thin sections. As seen in most thin sections, the opaque minerals are confined to the matrix, and they are typically intergrown with pyroxene. This texture suggests that both the pyroxene and opaque phases crystallized late in the paragenetic sequence.

Glass is a significant component of only a few thin sections. Where present, it forms intergranular masses between plagioclase crystals, thin linings on the walls of vesicles, and, rarely, rounded masses as much as 3 mm in diameter. The glass is typically charged with small blades of pyroxene as long as 0.5 mm and opaque minerals less than 0.1 mm in longest dimension.

#### PETROGRAPHY AND STRATIGRAPHY OF LAVA FLOWS

##### Group A

Flow 1: Two lava flows (flows 1 and 1A) that have been noted only in drill core 77-1 at the north end of the RWMC constitute group A. Field relations indicate that flows 1 and 1A are flow units of the tongue of basalt that was erupted from Quaking Aspen Butte and flowed down the valley of the Big Lost River in the area north of the RWMC (see Kuntz, 1978a). In drill core 77-1, the flows of group A are overlain by eolian clay, silt, and sand 1.4 m thick. Flows 1 and 1A are 10.4 m and 1.8 m thick respectively. The top of Flow 1 consists of dark- to medium-gray, fine-grained basalt containing as

much as 30 volume percent of round- to irregular- shaped vesicles as much as 3 cm in longest dimension. The top of the flow also has sediment-filled fractures. Within 1 m of the top of flow 1, equant to rounded crystals of olivine (to 2 mm) and slender laths of plagioclase (to 2 mm) are set in a matrix of olivine, plagioclase, and subophitic pyroxene, slender needles of ilmenite, and equant crystals of magnetite, all less than 0.5 mm in longest dimension. The rock is distinctly vesicular and diktytaxitic.

The middle of flow 1 consists of dark- to medium-gray, dense diktytaxitic slightly fractured basalt that has a few horizontal layers of nearly spherical vesicles that reach diameters of 2 cm. As seen in thin section, most laths of plagioclase are 1-2 mm long, the pyroxene is intergranular and 1-2 mm across, and ilmenite needles are as long as 1 mm. Near the base, as seen in hand specimen, the basalt is vesicular and equigranular. Plagioclase and olivine crystals are mostly <1 mm in longest dimension. Tiny crystals of ilmenite and magnetite are scattered through a cloudy matrix of anhedral pyroxene and some glass. The glassy matrix and olivine crystals are weakly to moderately oxidized.

The upper 1 m of flow 1A consists of reddish, oxidized, vesicular basalt that was obviously heated and altered by flow 1. The vesicles constitute as much as 35 percent of the rock and have an average diameter of about 1 cm. As seen in thin section, wedge-shaped, rectangular, and square olivine crystals as long as 1.5 mm and plagioclase phenocryst laths as long as 3 mm are set in a fine-grained, opaque, glassy matrix charged with dusty opaque material.

The size and shape of the olivine and plagioclase crystals in flows 1 and 1A are similar, and they suggest that the two flows were erupted from the same vent. Field relations indicate that flows 1 and 1A were erupted from Quaking Aspen Butte, approximately 20 km southwest of the RWMC in sec. 29, T. 1 N., R. 28 E.

## Group B

Three lava flows constitute group B: flows 2, 3, and 4. Flows 2 and 3 were penetrated by all 5 drill holes, but flow 4 was cut only by drill hole 93A (fig. 3). Flow 2 is immediately beneath the surficial cover in 4 of the drill cores and is overlain by surficial sediment and by flows and 1A in drill core 77-1 (fig. 3). The surficial sediment overlying flow 2 ranges in thickness from 1.8 m in drill core 77-1 to 7.3 m in drill core 95. The sediment is sand, silt, and clay of eolian and alluvial origin. Flows 2 and 3 are not separated by a sediment layer, but because the top of flow 3 is oxidized in most of the drill cores, flow 3 probably had cooled and solidified before flow 2 was emplaced. Flows 3 and 4 are separated by sediment about 0.9 m thick in drill core 93A. The sediment layer consists of clay mixed with basalt fragments and cinders that have a vitreous crust. We interpret the sedimentary interbed to be a local alluvial or lacustrine unit deposited within a short time (weeks or months, possibly a few years).

Field relations indicate that flow 2 was erupted from vent 5206, approximately 5 km southeast of the RWMC in sec. 32, T. 2 N., R. 29 E. The petrographic similarity of flows 2, 3, and 4 suggests that all erupted from the same vent.

Flow 2: Flow 2 ranges in thickness from 8.7 m in drill core 93A to 20.5 m in drill core 76-6. The upper several meters of the flow is clinkery, cindery, vesicular, much-fractured basalt. Many of the vesicles and fractures are filled with loess and caliche. Vesicles are irregular to subrounded and constitute from 20 percent to 40 percent of the upper 1 m of the flow. As seen in thin section, the rock is relatively equigranular. Equant olivine crystals are about 0.3 mm across and plagioclase laths are <1 mm long. Clinopyroxene is intergranular and <1 mm across, ilmenite needles are <0.5 mm

long. The rock is partly diktytaxitic and contains small amounts of intergranular glass.

The middle part of the flow is dark-gray, massive basalt that is equigranular near the top and progressively more porphyritic toward the bottom. The porphyritic phase consists of olivine and plagioclase phenocrysts and glomeroporphyritic clots of olivine and plagioclase set in an intergranular matrix of olivine, plagioclase, clinopyroxene, and opaque minerals. Olivine phenocrysts are as large as 2.5 mm across, and laths of plagioclase are as large as 1.5 mm in length. In the matrix, olivine, plagioclase, intergranular clinopyroxene, magnetite, and ilmenite crystals are all <0.5 mm across. The rock is distinctly diktytaxitic.

The bottom several meters of the flow consists of dark gray, vesicular, cindery basalt. Vesicles are round, and they occupy as much as 20 percent of the rock volume. As seen in thin section, the rock is distinctly porphyritic; it contains equant olivine phenocrysts as large as 1.5 mm in diameter. These phenocrysts are oxidized on crystal faces and along fractures. Plagioclase laths are as long as 4 mm. Olivine and plagioclase phenocrysts are set in a matrix of olivine, plagioclase, subophitic clinopyroxene, and ilmenite and magnetite crystals that are all <0.6 mm in longest dimension. Several thin sections examined from this horizon are of porphyritic rock that contains phenocrysts of olivine and plagioclase  $\geq 1$  mm in longest dimension set in a matrix of the same minerals, plus clinopyroxene and opaque minerals that are all <0.1 mm in longest dimension. Sheafs and swallow-tail bundles of plagioclase laths are ubiquitous.

Flow 3: Flow 3 ranges in thickness from 10 m in drill core 95 to 6 m in drill core 77-1. The upper meter of the flow is fine-grained, brownish-red to purplish-gray, and moderately to strongly oxidized. Rounded to irregular

vesicles as much as 8 mm in longest dimension occupy as much as 30 percent of the rock volume. In thin section, the rock is seen to have equant olivine crystals ranging from 0.5 to 1 mm across and slender plagioclase laths as long as 4 mm set in an intergranular matrix of clinopyroxene, plagioclase, olivine, ilmenite, and magnetite crystals, all <0.8 mm in greatest dimension, and minor amounts of glass.

The middle part of the flow consists of slightly fractured dark-gray, diktytaxitic, dense to slightly vesicular basalt. Vesicles, scattered throughout the rock and concentrated in vertical to nearly vertical vesicle pipes, are typically round and less than 2 mm in size; they constitute less than 3 percent of the rock volume. The rock is distinctly porphyritic as seen in thin section; it has equant phenocrysts of olivine as large as 1.2 mm across and plagioclase laths as long as 3 mm set in a matrix of olivine, plagioclase, intergranular to subophitic clinopyroxene, and ilmenite and magnetite crystals, all <0.5 mm in longest dimension. Distinctive features are glomeroporphyritic clots of plagioclase crystals in swallow-tail sheafs and clots of olivine and plagioclase crystals.

The bottom meter of the flow is reddish-brown, oxidized, vesicular, distinctly porphyritic basalt. Phenocrysts of plagioclase as long as 2 mm are set in a matrix of olivine, plagioclase, subophitic clinopyroxene, and opaque crystals, all <1 mm long. The glomeroporphyritic clots of plagioclase crystals and plagioclase-olivine crystals, typical of the middle of the flow, are also present at the base of the flow.

Flow 4: Flow 4, recognized only in drill core 93A, is 4.3 m thick. The top of the flow is dark gray, fine-grained, and vesicular, and it contains fractures filled with clay. The vesicles are as large as 2 cm, and they

constitute as much as 10 percent of the volume of the rock. The middle and bottom of the flow are dark-gray, fine-grained, slightly vesicular, diktytaxitic basalt. In thin section, the middle of the flow is seen to be moderately porphyritic and to contain crystals of equant olivine as large as 1.5 mm across and slender laths of plagioclase as long as 2 mm set in a matrix of olivine, plagioclase, intergranular clinopyroxene, ilmenite, and magnetite crystals, all <0.5 mm long. Sheafs and bundles of plagioclase crystals are typical of this flow.

The porphyritic character of flows 2, 3, and 4, all having olivine and plagioclase phenocrysts set in a typically intergranular matrix, along with the sheafs and bundles of plagioclase laths, suggests that all three flows were erupted from the same vent, designated as vent 5206, located approximately 5 km SSE of the RWMC in sec. 32, T. 2 N., R. 29 E. (See Kuntz, 1978a.)

#### Group C

Flows in group C are separated from the flows of group B by a sedimentary interbed that ranges in thickness from 0.3 m to 7.9 m (Barraclough and others, 1976). Group C consists of flows 5, 6, and 7. All flows appear in all 5 of the drill cores, and none of the flows is separated by sedimentary interbeds. Flow 6 has been subdivided into 2 flow units (flows 6A and 6B) in drill core 76-6; flow 7 has been subdivided into 2 flow units (flows 7A and 7B) because of distinct flow breaks in drill cores 94, 95, 77-1, and 76-6.

Flow 5: Flow 5 ranges in thickness from 4.5 m in drill core 93A to 12.2 m in drill core 95. The top several meters of flow 5 consists of dark-gray, fine-grained, diktytaxitic, vesicular basalt. Vesicles are round to

irregular in shape, as long as 1.5 cm, and constitute as much as 30 percent of the rock volume. Thin coatings of clay and carbonate mineral(s) line vesicle walls and fracture surfaces. As seen in thin section, the rock is characterized by distinctive ophitic laths of clinopyroxene as long as 2 mm. Olivine crystals as long as 1.5 mm and plagioclase crystals as long as 2 mm are sparse. Clots of 4 or 5 olivine crystals and cross-shaped clots of plagioclase are present. The matrix consists mostly of olivine, plagioclase, and subophitic clinopyroxene crystals <1.0 mm in longest dimension. Magnetite and ilmenite crystals are <0.4 mm long.

The middle of the flow is medium-gray, diktytaxitic, massive basalt that contains a few small (<1 cm) vesicles and rare fractures. As seen in thin section the rock is characterized by ophitic blades of clinopyroxene as long as 1.5 mm. Olivine occurs as single crystals as large as 2.5 mm, as clots of 3 or 4 crystals, and as smaller (<0.5 mm) crystals in the matrix. Some plagioclase crystals are as long as 2 mm, but most are <0.5 mm and are confined to the matrix. The clinopyroxene occurs both as the larger ophitic crystals and as intergranular crystals <0.5 mm across in the matrix. Magnetite and ilmenite crystals form opaque masses and intergrowths with the clinopyroxene of the matrix.

The base of the flow is brownish- to reddish-gray, cindery, clinkery basalt that is variably oxidized. As seen in thin section, the rock has single olivine crystals as large as 3.5 mm and clots of several grains the same size. Several thin sections contained olivine with opaque coatings on crystal faces and on fracture surfaces. Some plagioclase crystals are as long as 2.5 mm, but most are only 0.5 to 1 mm long and are part of the matrix. Clinopyroxene crystals 1 to 2 mm long are ophitic; crystals <1 mm long in the matrix are subophitic. Magnetite and ilmenite crystals are <0.5 mm long.

Flow-6: Flow 6 ranges in thickness from 3.4 m in drill core 95 to 11.9 m in drill core 94. The upper 0.5 to 3 m of the flow consists of reddish, oxidized, scoriaceous, vesicular basalt. Vesicles are irregular in shape and constitute as much as 30 percent of the rock volume. In thin section, the rock is seen to have distinctive clots of partly oxidized olivine and phenocrysts of ophitic clinopyroxene. The clots contain from 6 to 12 equant olivine crystals, some as large as 3 mm across. Plagioclase laths as long as 2 mm are typically arranged in sheafs, bundles, and cross-shaped clots. Anhedral clinopyroxene crystals as long as 3 mm are ophitic, but smaller crystals <1 mm are subophitic. The matrix consists of olivine, plagioclase, subophitic clinopyroxene, magnetite, and ilmenite crystals all <1 mm. The rock contains some glass and is diktytaxitic.

The middle of the flow is more massive and dense than the upper part, contains a few nearly spherical vesicles, and is typically purplish-gray. In thin section, the rock is seen to be porphyritic; olivine, plagioclase, and ophitic clinopyroxene crystals >2 mm long are set in a matrix of the same three minerals plus magnetite, ilmenite, and some glass, all of which are <1 mm long. The olivine crystals form clots of 3 to as many as 10 crystals; the larger crystals are 1.2 to 1.6 mm in diameter. Smaller matrix crystals (<0.3 mm) in some samples are altered, causing the purplish hue of hand specimens. Plagioclase crystals are rarely as long as 3 mm, and most are <2 mm. Sheafs and bundles of crystals are typical. Clinopyroxene occurs as ophitic crystals as large as 3 mm and as subophitic crystals <1 mm long in the matrix. Ilmenite blades are as long as 0.6 mm, and magnetite crystals are <0.5 mm in diameter.

The bottom meter of the flow is brownish-gray to grayish-red, scoriaceous, vesicular basalt. In thin section, the rock looks much like that in the middle and top of the flow. Clots and individual crystals of equant olivine are as large as 3 mm across. Plagioclase laths are as long as 2 mm, but most crystals are <1 mm, and many crystals are arranged in sheafs and bundles. Ophitic crystals of clinopyroxene are as long as 2 mm, and subophitic crystals are <1 mm. The rock is diktytaxitic but contains some glass. Olivine crystals in the matrix are variably altered.

Because of a distinct cooling break in the middle of flow 6 at a depth of 50 m in drill core 76-6, we have subdivided flow 6 into two flow units, flows 6A and 6B, in that drill core. The macroscopic and microscopic features of flow 6A are nearly identical with those of flow 6. In thin section, flow 6B is distinguished by glomeroporphyritic clots each consisting of 3 to 10 olivine crystals. At the top of flow 6B, all the clinopyroxene is part of the fine-grained matrix and is intergrown with some glass and feathery opaque minerals. Near the bottom of flow 6B, the clinopyroxene is subophitic to ophitic, and crystals are as long as 2.5 mm. Glomeroporphyritic sheafs and bundles of plagioclase are as long as 2 mm in both the top and bottom of the flow.

Flow 7: Flow 7 and its subdivisions 7A and 7B together range from 15.7 m thick in drill core 94 to 22.9 m thick in drill core 93A. As shown in figure 3, cooling breaks were noted in all drill cores except 93A. Thus, flow 7 was divided into two flow units 7A and 7B in four of the five drill cores. The top several meters of flow 7 in drill core 93A and of flow 7A in the other 4 drill cores consists of reddish-gray to purplish-gray, strongly oxidized, fine-grained basalt. It contains abundant spherical vesicles 1 to

5 mm in diameter that constitute as much as 20 percent of the rock volume. Thin sections show strong alteration of both large and small olivine crystals and variable development of ophitic texture. Equant, single crystals and glomeroporphyritic clots of as many as ten olivine crystals are conspicuous. Plagioclase crystals are all <1.5 mm long, and many of the larger crystals form bundles. Anhedral ophitic clinopyroxene crystals are as long as 3.2 mm. Most thin sections show patchy subophitic crystals <1 mm. Rare ilmenite blades are as long as 1 mm and magnetite is <0.5 mm.

The middle part of flow 7A and the upper part of flow 7 consist of brownish-gray, dense, slightly vesicular basalt containing a few nearly vertical fractures partly filled with clay. The rock as seen in thin section varies in texture from coarse-grained and equigranular to porphyritic, and it contains large, single crystals of olivine and glomeroporphyritic clots of olivine crystals or phenocrysts. Equant olivine crystals are as long as 4 mm, and clots contain as many as ten crystals. Olivine crystals in the matrix are <0.5 mm across and are weakly to strongly altered. Most plagioclase crystals are <1 mm long, and cross- and x-shaped clots of plagioclase are common. Ophitic laths of clinopyroxene are as long as 3.2 mm, but most crystals are 0.7 mm to 2 mm in longest dimension. Magnetite forms square, rectangular, and irregular-shaped crystals <0.4 mm long. Rare ilmenite needles are as long as 0.4 mm.

The bottom of flow 7A is brownish-gray, slightly vesicular, dense basalt. Its petrographic character is much like that of the middle of the flow except that the rock is distinctly porphyritic. Phenocrysts of olivine as large as 2 mm across are set in a matrix of olivine, plagioclase, and subophitic clinopyroxene, all <1 mm in longest dimension. Smaller olivine

crystals are altered to reddish material along cleavage planes, and crystal surfaces are veneered by opaque minerals.

The top half meter of flow 7B is reddish-gray, scoriaceous, and strongly vesicular. These characteristics indicate a flow break. In thin section, the rock shows variable textures. Several thin sections were cut from coarse-grained rocks in which single crystals and clots of olivine are as large as 3.5 mm. Anhedral, ophitic clinopyroxene crystals as long as 3.5 mm are set in a matrix of plagioclase laths, subophitic clinopyroxene, and sparse olivine. All components of the matrix are <0.5 mm in longest dimension. Slender needles of ilmenite reach 1.5 mm in length, and abundant magnetite crystals are  $\leq 0.5$  mm across. Other thin sections of equigranular rocks contain plagioclase laths, subophitic clinopyroxene crystals and single crystals and clots of 6 to 10 olivine crystals, all <1 mm in longest dimension. Olivine is altered to reddish-brown material, and calcite is abundant in rocks of both textural types.

The middle part of flow 7B consists of brownish-gray, weakly vesicular basalt that contains numerous clay-filled fractures. In thin section, the rock shows variable textures. Some thin sections of coarse-grained rocks contain single crystals and clots of olivine crystals as large as 3.5 mm. Subhedral laths of ophitic clinopyroxene are as long as 2 mm, plagioclase laths are as long as 2 mm and are arranged in star-shaped clusters, ilmenite blades are as long as 2 mm, and equant crystals of magnetite are  $\leq 0.4$  mm across. Other thin sections contain clots of olivine crystals  $\leq 1.5$  mm across, slender laths of plagioclase 0.2 to 0.7 mm long, subophitic laths and granules of clinopyroxene <1 mm in longest dimension, and ilmenite and magnetite crystals <0.4 mm across.

The bottom of flow 7B is brownish-gray, dense, distinctly porphyritic, diktytaxitic, slightly vesicular basalt. Most of the vesicles are alined in vertical trains. Single olivine crystals as long as 5 mm and clots of 3 to 10 crystals are common. Plagioclase laths are typically <1.5 mm long. Clinopyroxene is subophitic, anhedral, and <1 mm in longest dimension. Magnetite and ilmenite crystals are <0.5 mm in longest dimension. In samples from near the base, olivine crystals are oxidized to reddish-brown material along fractures and to opaque material on crystal faces.

All flows in group C are characterized by glomeroporphyritic olivine crystals 2-5 mm across, distinctive, ophitic clinopyroxene 1-3 mm in longest dimension, and relatively small (<1.5 mm long) plagioclase crystals. Together with the absence of major sedimentary interbeds between flows, these similarities suggest that the flows were all erupted from the same vent or from vents which tapped the same magma source.

#### Group D

Flow 8: Group D consists of a single lava flow, flow 8. Flow 8 is overlain by the thickest sedimentary interbed penetrated in the drill cores. The thickness of the interbed, as much as 6.5 m, suggests a significant time interval between groups C and D. Only two of the five drill cores examined in this study completely penetrated flow 8; the thickness of the flow is 8.5 m in drill core 94 and 10.0 m in drill core 77-1. Broken, sediment-coated fragments of dark-gray basalt near the middle of flow 8 in drill core 77-1 may indicate a flow break. However, evidence for a flow break was not found in drill core 94, so we did not subdivide flow 8 into separate flow units.

The top meter of flow 8 is dark-gray basalt that contains round and irregular vesicles about 3-5 mm in longest dimension. These vesicles

constitute as much as 35 percent of the rock volume. In thin section, the rock is seen to be porphyritic. It has plagioclase phenocryst laths as long as 2.5 mm set in a matrix of rounded, subhedral olivine crystals, intergranular clinopyroxene, plagioclase, ilmenite, magnetite, and some glass, all <1 mm in longest dimension.

The middle part of the flow typically is dense, diktytaxitic gray basalt that contains only scattered, rounded vesicles <2 mm in diameter. In thin section, the rock looks much like the part near the top of the flow, except that plagioclase phenocrysts reach lengths of as much as 3 mm, and many crystals form bundles.

Near the base of flow 8, the rock is dark gray and diktytaxitic. Many irregular to round vesicles 2-8 mm in longest dimension constitute as much as 30 percent of the rock volume. In thin section, the rock looks much like the upper part of the flow, except that the clinopyroxene is very fine-grained intergranular material that is intergrown with fine, dusty opaque minerals.

The remaining groups of lava flows (E, F, G) were penetrated only by drill hole 77-1 and, thus, their extent and variations in thickness are unknown. All the following descriptions refer only to observations of drill core 77-1.

#### Group E

Flow 9: Group E is a single lava flow (flow 9) 23 m thick. The flow is separated from flow 8 by a sediment interbed 1 m thick. Flow 9 contains apparent minor flow breaks 4.9 m and 18.6 m below its top. These breaks are thin (<0.5 m) zones where the basalt is more vesicular and rubbly but not strongly oxidized. They may well have been caused by differential flow between layers in a single flow, and we conclude that flow 9 is, in fact, a

relatively thick single flow. The upper 2 m of the flow is reddish-brown to brownish-gray basalt that contains round to irregular vesicles as large as 1 cm in diameter; vesicles constitute 15 to 20 percent of the rock volume. In thin section, the rock is seen to vary texturally from porphyritic to equigranular. Olivine and rare plagioclase phenocrysts 1 to 1.5 mm long are set in an intergranular matrix with anhedral, patchy, ophitic crystals of clinopyroxene as long as 2 mm. In both textural varieties, the olivine crystals are euhedral and equant, and they form clots of 3 or 4 grains. Plagioclase laths are typically <0.5 mm long, and opaque minerals are all <0.1 mm in maximum diameter. The rock is diktytaxitic, but it contains some glass and ubiquitous calcite in vesicles.

The middle of flow 9 has a varied texture that ranges from dense and diktytaxitic to fractured, jointed, and strongly vesicular. The diktytaxitic variant is dark gray; the vesicular variant is brownish-gray. The vesicles range in size and shape from about 1 mm in diameter and round to as large as 1.5 cm and irregular. The vesicles form horizontal layers and vertical trains, and they constitute as much as 35 percent of the rock volume. As seen in thin section, the texture of the middle part of the flow is depth-dependent; the pyroxene is distinctly intergranular near the top, becomes subophitic near the middle, and is distinctly ophitic at the base. Olivine crystals are equant and euhedral, and they range in size from phenocrysts as large as 1.5 mm down to grains in the matrix that are <0.5 mm. The plagioclase crystals are very slender (length-width ratio of 20:1) and are <1 mm long. Many form cross-shaped clots and glomeroporphyritic arrangements with olivine. The rock is uniformly diktytaxitic. Olivine crystals are slightly oxidized, and calcite is widely dispersed in vesicles and as fracture fillings.

The bottom meter of flow 9 is brownish-gray, fine-grained, rubbly, vesicular basalt. Mainly irregular vesicles about 1-3 cm in longest dimension constitute as much as 35 percent of the rock volume. As seen in thin section, the rock is fine-grained (all crystals <1 mm) and non-porphyrific and consists of olivine, slender needles of plagioclase, and intergranular to subophitic granules of clinopyroxene. Intergranular masses of opaque minerals are typically intergrown with clinopyroxene.

#### Group F

Three flow units (flows 10A, 10B, and 10C) and flow 11 compose group F. Group F is separated from flow 9 above by reddish-orange to brown, silty clay, a meter thick. This interbed was baked by flow 9. Flow 10 is 39.6 m thick, but it has significant flow breaks at depths of 3.2 m and 22.2 m below its top. Thus, flow 10A is 3.2 m thick, flow 10B is 19 m thick, and flow 10C is 17.4 m thick. The rock immediately beneath each of the flow breaks is highly vesicular, rubbly, and oxidized to a reddish-brown color. These features indicate that the two lower flow units had cooled and were baked by the overlying flow unit.

Flow 10: The upper half of flow 10A consists of reddish-gray, rubbly basalt containing numerous, nearly spherical vesicles <1 cm in diameter. The rock contains many open voids and cracks filled with gray, silty clay derived from the overlying sedimentary interbed. The bottom half of the flow is dark-gray, massive, diktytaxitic basalt that has a few small (<5 mm) rounded vesicles and randomly oriented fractures. A single thin section from the middle of flow 10A shows the rock to be porphyritic and to contain plagioclase laths 2 mm to 3.5 mm long. Many of the plagioclase crystals are arranged in sheafs and bundles. The matrix consists of rounded olivine crystals <0.8 mm

in diameter, scattered plagioclase crystals <1 mm in length, clinopyroxene as subophitic blades as long as 1 mm and as intergranular crystals mostly <0.5 mm, ilmenite needles as long as 0.6 mm, and magnetite crystals <0.2 mm across.

The top of flow 10B is reddish- to brownish-gray, fine-grained basalt that contains irregular-shaped vesicles 1-10 mm in longest dimension. The vesicles constitute as much as 40 percent of the rock volume. As seen in thin section, the rock is porphyritic; phenocrysts of plagioclase as long as 2 mm are set in a matrix of olivine granules, plagioclase laths, intergranular clinopyroxene, ilmenite, and magnetite crystals, all <0.5 mm.

The middle of flow 10B is chiefly brownish-gray, dense to slightly vesicular basalt that contains widely dispersed, randomly oriented fractures. As seen in thin section the rock ranges texturally from varieties similar to that described immediately above to coarse-grained rock. The coarse-grained rock consists of equant olivine crystals as large as 2 mm, slender plagioclase laths with length to width ratios of as much as 20:1 that are 0.5 mm to 2.5 mm long, ophitic and twinned clinopyroxene crystals as long as 3 mm, ilmenite blades as long as 1.2 mm, and magnetite crystals that are <0.4 mm. The rock is hypocrystalline and contains irregular to rounded patches of glass charged with minute opaque crystals. A thin section from a sample 1 m above the base of flow 10B is nearly identical in texture with the section from the top of the flow except that olivine crystals in the matrix are strongly altered to reddish-brown material along fractures and on crystal surfaces.

The top 2 m of flow 10C consists of reddish-brown, fine-grained, vesicular basalt. Irregular vesicles 5 mm to 20 mm in longest dimension

constitute as much as 20 percent of the rock volume. The rock in thin section is seen to contain olivine granules, plagioclase laths, clinopyroxene granules and subophitic blades, and ilmenite and magnetite crystals that are all <1 mm in longest dimension. The olivine is altered to reddish-brown material.

The middle of flow 10C is light-gray, largely massive, dense basalt, but it locally contains small rounded vesicles 1 mm to 5 mm across that are arranged in horizontal layers as much as 5 cm thick. As seen in thin section the rock consists of anhedral clinopyroxene as long as 2 mm, plagioclase single crystals and glomeroporphyritic clots as long as 3.2 mm, olivine granules  $\leq 0.5$  mm across, ilmenite blades 0.5 mm to 1 mm long, and magnetite crystals that are  $\leq 0.5$  across. The rock also contains large plagioclase crystals that have sieve texture and wormy cores.

At the base of flow 10C, the rock is dark brownish-gray and contains clay-lined fractures and irregular-shaped vesicles as much as 2 cm long. In thin section the rock is nearly identical to that described for the middle of the flow except that all crystals are <2 mm in longest dimension.

Flow 11: Flow 11 is 17.8 m thick. The upper 3 m of flow 11 is reddish-brown, vesicular, diktytaxitic basalt. Vesicles are irregular in shape, are 3 mm to 20 mm in longest dimension, and constitute as much as 15 percent of the rock volume. The texture of the rock as seen in thin section is fine-grained and nonporphyritic. Equant olivine crystals are  $\leq 0.4$  mm across, and clots of 3 to 8 crystals about 0.2 mm across are common. Plagioclase laths are all <1 mm long, and many are arranged in bundles or sheafs. Clinopyroxene occurs in anhedral, subophitic crystals <1.2 mm in longest dimension. Ilmenite blades and magnetite crystals are <0.5 mm in longest dimension.

The middle of the flow is medium-gray to purplish-gray, diktytaxitic, dense basalt. It contains a few small (<5 mm), rounded vesicles arranged in both horizontal layers and vertical pipes. The few fractures are mainly horizontal or vertical. The texture coarsens toward the center of the flow, then becomes finer toward the base. A thin section from a sample at the center of the flow is coarse-grained and contains irregular ophitic crystals of clinopyroxene as large as 4 mm in longest dimension, plagioclase laths as long as 3 mm, olivine granules <1 mm across, slender ilmenite needles as long as 3 mm, and magnetite crystals  $\leq 1$  mm across.

At the base of the flow, brownish-gray, fine-grained, diktytaxitic rock contains round vesicles 0.5 mm to 1 mm in diameter. The walls of the vesicles are stained orange-brown. As seen in thin section, the rock is fine-grained and contains olivine single crystals and glomeroporphyritic clots  $\leq 1$  mm across. The remaining minerals are intergranular clinopyroxene, plagioclase <0.5 mm in size, and opaque minerals  $\leq 0.1$  mm across.

Flows 10A, 10B, 10C, and 11 all are characterized by ophitic clinopyroxene and plagioclase laths typically >2 mm in length in the central parts of flows, relatively small olivine single crystals and clots of olivine crystals <1 mm, and blades of ilmenite  $\leq 3$  mm long. The similarity of these characteristics in all four flow units suggests that all were erupted from the same vent or from several vents that tapped the same magma source.

#### Group G

Two flows (flow 12, flow 13) make up group G. Flow 12 is separated from flow 11 by orange-brown silty clay 0.3 m thick. Flow 12 is 6.1 m thick, and flow 13 is at least 7.3 m thick. Drill core 77-1 bottomed probably near the middle of Flow 13 at a depth of 182.9 m.

Flow 12: The upper 3 m of flow 12 is brownish-gray, fine-grained, diktytaxitic basalt that contains rounded vesicles as large as 1 cm in diameter. As seen in thin section, the rock contains a few large olivine crystals as long as 2 mm, but most crystals are 0.4 to 1.2 mm long. Plagioclase laths are all <1 mm, and many are arranged in sheafs and bundles. Clinopyroxene occurs as intergranular crystals <0.3 mm in greatest dimension and as subophitic laths as long as 0.6 mm. Opaque minerals are all <0.1 mm in greatest dimension. They are chiefly scattered throughout intergranular patches of glass.

The middle of flow 12 is medium-gray to brownish-gray, diktytaxitic, chiefly dense basalt that is nearly free of vesicles and fractures. As seen in thin section, the rock is coarse-grained and non-porphyrific. Single crystals and clots of 3 or 4 olivine crystals are 0.5 to 3 mm in longest dimension. Plagioclase laths are <1.5 mm long, intergranular to subophitic crystals of clinopyroxene are <0.5 mm in longest dimension, and opaque minerals are ≤0.4 mm across.

At the base of flow 12, the rock is brownish-gray and diktytaxitic. It contains round to irregular vesicles as large as 1 cm across that constitute as much as 20 percent of the rock volume. The rock, as seen in thin section, is almost identical to that described above for the middle of the flow.

Flow 13: The upper 2.5 m of flow 13 is reddish-brown to grayish-brown, diktytaxitic basalt that contains randomly oriented fractures. Irregular-shaped vesicles  $\leq 1$  cm in longest dimension occupy about 15 percent of the rock volume.

At a depth of 6 m below the top of flow 13, the rock is dark gray, fine-grained, dense basalt that is nearly free of vesicles and fractures. In thin section, the rock is seen to be porphyritic with phenocrysts of equant olivine crystals as long as 2 mm and ophitic crystals of clinopyroxene as large as 2.5 mm. These crystals are set in a matrix of olivine granules, plagioclase laths, subophitic clinopyroxene, ilmenite, and magnetite crystals, all  $\leq 1.2$  mm in greatest dimension.

#### Correlations of flows with source vents

Attempts to correlate the lava flows in the drill cores with source vents in the Arco-Big Southern Butte area have proven difficult for several reasons. All lava flows cored by the drill are extremely similar in both megascopic and microscopic characteristics, as is clear from the foregoing petrographic descriptions. This difficulty is compounded by the fact that surface lavas in the Arco-Big Southern Butte area are also remarkably similar in their microscopic characteristics.

The correlations of flows in group A with a source vent at Quaking Aspen Butte, and of flows in Group B with a source at Vent 5602 (sec. 32, T. 2 N., R. 29 E.; see Kuntz, 1978a) are based on geological field relations, i.e., the flows can be traced visually to their source vents on the bases of their morphology and distribution. For the reasons cited above, correlations of lava flows of groups C through G with possible source vents would probably be

wrong. Such tentative correlations would add little to our evaluation of volcanic hazards for the RWMC.

## K-Ar DATING

### Analytical techniques

Thin sections of 102 samples of basalt from three of the five drill cores (94, 77-1, 76-6) were examined petrographically to determine those most suitable for K-Ar dating. Of these samples, 19 were chosen for analysis, representing all flows except numbers 4, 10, and 11. The chosen samples included 2 from drill core 94, 5 from drill core 76-6, and 12 from drill core 77-1. The locations of the dated samples are shown on fig. 3. All analyzed samples met the usual criteria of acceptability for whole-rock K-Ar dating (Dalrymple and Lanphere, 1969; Mankinen and Dalrymple, 1972). The final selection of samples was based not only on their petrographic suitability but also on their distribution among the identified flows and groups and among the three drill cores. No samples from flows 4, 10, or 11 were suitable for dating.

The samples were first crushed with a jaw crusher, then passed through a hardened steel roller mill, and finally sieved with stainless steel sieves to a size of 1 to 2 mm. An aliquant (10 grams) of this sized master sample was pulverized to less than 74  $\mu\text{m}$  with a pulverizer that had hardened steel crucibles and pucks. This powdered material was used for the  $\text{K}_2\text{O}$  measurements. Aliquants of the remaining 1-2 mm material were used for the Ar analyses. All aliquants were split from the master sample, and the  $\text{K}_2\text{O}$  powder sample was split with a Jones-type microsplitter.

Potassium was measured by flame photometry with the lithium metaborate fusion technique (Ingamells, 1970) and appropriate standards. Two 0.5-gram

aliquants were split from each  $K_2O$  powder, and duplicate  $K_2O$  measurements were run for each split; thus a total of 4  $K_2O$  measurements were made for each dated sample. An abundance of  $1.167 \times 10^{-4}$  mole  $^{40}K$ /mole K (Garner and others, 1975) was used to calculate the quantity of  $^{40}K$  from the  $K_2O$  results.

Radiogenic  $^{40}Ar$  was measured by isotope dilution mass spectrometry according to techniques described by Dalrymple and Lanphere (1969). Two aliquants of each sample were independently extracted and measured (table 1, extr. nos. 1, 2). The samples, which ranged in size from 16 to 27 grams, were placed in prefired molybdenum crucibles and baked overnight in ultra-high-vacuum extraction lines at  $280^\circ C$ . Fusion was by induction heating using 7.5-kW and 10-kW radio frequency generators. During fusion an  $^{38}Ar$  tracer of known isotopic composition and amount was introduced and mixed with the sample gas. Reactive gases, including  $H_2$ ,  $O_2$ ,  $N_2$ , and  $CO_2$ , were removed by reaction with hot  $CuO$  ( $450^\circ C$ ) and Ti metal ( $800^\circ C$ );  $H_2O$  was absorbed with a 5-Å artificial zeolite molecular sieve. After purification, the argon was collected in breakseal tubes by absorption on activated charcoal cooled by liquid nitrogen and was analyzed with a mass spectrometer.

Two separate  $^{38}Ar$  tracer systems, M and N, were used in the measurements, as indicated in table 1. Both are bulb tracers and contain high-purity  $^{38}Ar$  ( $\gg 99$  percent). Their  $^{38}Ar$  concentrations are traceable, through standards, to absolute air Ar calibration, and their calibrations are frequently checked with intralaboratory standards. Interlaboratory comparisons of argon determinations of the U.S. Geological Survey's Menlo Park, Calif., laboratory with those of other geochronological laboratories throughout the world can be found in Lanphere and Dalrymple (1976). Uncertainties in the composition and absolute concentrations of the Ar isotopes and in the bulb depletion constants contribute negligible errors to the Ar analyses in this study.

Mass analyses were done with a single-collector, first-order, direction-focusing mass spectrometer with a  $60^\circ$  sector magnet and a 15.24-cm radius. The instrument utilizes a dedicated minicomputer for magnet field control, data acquisition, and on-line data reduction. For many of the samples, duplicate mass analyses were done on the sample gas from each extraction (mass analyses A, B, and C, in table 1). These replicate  $^{40}\text{Ar}/^{38}\text{Ar}$  ratios have a pooled estimate of the standard deviation of precision ( $S_p$ ) of 0.07 percent with 95-percent confidence limits of 0.055 percent and 0.097 percent. For the replicate  $^{38}\text{Ar}/^{36}\text{Ar}$  ratios,  $S_p$  is 0.48 percent with 95-percent confidence limits of 0.38 percent and 0.66 percent. The  $^{38}\text{Ar}/^{36}\text{Ar}$  ratios are less precise than the  $^{40}\text{Ar}/^{38}\text{Ar}$  ratios because the  $^{36}\text{Ar}$  signal is typically two to three orders of magnitude smaller than either the  $^{40}\text{Ar}$  or  $^{38}\text{Ar}$  signals. The median difference between replicate  $^{40}\text{Ar}/^{38}\text{Ar}$  measurements is 0.025 percent with 90 percent of the replicates agreeing to better than 0.1 percent (fig. 4). The median difference between replicate  $^{38}\text{Ar}/^{36}\text{Ar}$  ratios is 0.015 percent with 90 percent agreeing to better than 0.2 percent.

The means of the replicate gas compositions (mass analyses A, B, and C in table 1) were used to calculate the amount of radiogenic  $^{40}\text{Ar}$  in each sample extracted. The pooled estimate of precision of the radiogenic  $^{40}\text{Ar}$  analyses on those duplicate argon extractions with radiogenic  $^{40}\text{Ar}$  contents greater than 1 percent (extr. nos. 1 and 2 in table 1) is 18.7 percent with 95-percent confidence limits of 13.2 percent and 31.79 percent. The primary reason that the precision of the duplicate extractions is much poorer than the precision of the argon ratios from the replicate mass analyses is because of the small percentage of radiogenic  $^{40}\text{Ar}$  in the samples and the error magnification that occurs when one relatively large number (the atmospheric  $^{40}\text{Ar}$ ) must be

Table 1. Potassium-argon age data for samples of basalt from drill holes at the Radioactive Waste Management Complex, Idaho  
National Engineering Laboratory, Idaho.

Argon

Flow	Sample No.	$K_2O^+$ (wt. %)	Extr. No.	Wgt. (gms)	Tracer	Mass Analysis		$^{40}Ar/^{38}Ar$	$^{38}Ar/^{36}Ar$	$^{40}Ar_{rad}$ (mol/gm)	$^{40}Ar_{rad}$ (percent)	A		B	
						No.	No.					Calculated Age (10 <sup>3</sup> years)	Weighted Mean* (10 <sup>3</sup> years)		
1	77-1-30	0.660 ± 0.002	2 <sup>a</sup>	15.809	N	{ A B }	0.6254	468.9	<1.0 x 10 <sup>-13</sup>	<1.0	<100	95 ± 50	<240	95 ± 50	
							0.6257	470.0							
2	76-6-64	0.698 ± 0.003	1	25.995	M	A	5.627	52.47	<2.7	<1.0	<270	<240	<240		
							5.026	58.67							
37	77-1-81	0.735 ± 0.002	1	19.731	M	A	4.018	73.35	<2.5	<1.0	<240	<200	<200		
							4.553	64.83							
3	76-6-90	0.685 ± 0.013	1	23.822	M	{ A B }	3.625	81.63	<1.9	<1.0	<190	<220	<190		
							3.622	81.59							
5	77-1-126	0.410 ± 0.004	1	26.060	M	{ A B }	4.406	66.96	<2.2	<1.0	290 ± 60	285 ± 70	290 ± 45		
							1.235	244.8							
	76-6-127	0.533 ± 0.003	1	24.060	M	{ A B }	1.521	197.6	1.730	2.9	<240	<330	<240		
							3.461	85.51							
	76-6-127	0.533 ± 0.003	1	24.060	M	{ A B }	3.458	85.60	<1.8	<1.0	<240	<330	<240		
							4.662	63.33							
2	22.903	M													

Argon

Flow	Sample No.	$K_2O^+$ (wt. %)	Extr. No.	Wgt. (gms)	Tracer	Mass Analysis		$^{40}Ar/^{38}Ar$	$^{38}Ar/^{36}Ar$	$^{40}Ar$ (mol/gm)	$^{40}Ar$ (percent)	A		B
						No.	No.					Calculated Age ( $10^3$ years)	Weighted Mean ( $10^3$ years)	
6	77-1-157	0.527 ± 0.003	1	24.935	M	A	1.366	218.7	1.257	1.8	165 ± 50	180 ± 35		
							B	1.367					218.8	
		2	26.193	M	A	1.334	226.0	1.542	2.4	200 ± 50				
						B	1.335						224.6	
	77-1-166.5	0.540 ± 0.003	1	25.654	M	A	1.820	169.0	1.360	1.5	175 ± 65	180 ± 50		
							B	1.817					164.5	
C							1.815	164.3						
7	BG-94-190	0.441 ± 0.002	1	26.409	M	A	2.036	146.8	1.492	1.5	190 ± 70			
							B	1.238					243.6	
		2	26.155	M	A	1.371	217.8	1.114	1.7	175 ± 60				
						B	1.371						217.7	
	76-6-210	0.395 ± 0.002	1	22.545	M	A	0.9045	332.3	1.429	2.8	250 ± 65	240 ± 45		
							B	0.9043					333.2	
77-1-181.5	0.498 ± 0.004	1	24.736	M	A	1.116	269.3	1.460	2.5	205 ± 45				
						B	1.115						269.9	
77-1-210.5	0.500 ± 0.002	1	23.622	N	A	1.035	291.2	0.858	1.3	120 ± 80				
						B	0.6486						455.5	
		2	26.258	M	A	1.035	291.2	1.392	2.8	195 ± 50				
						B	0.6481						457.6	
		2	25.536	N	A	0.4271	703.6	1.369	3.5	190 ± 75				
						B	0.4277						704.2	

Argon

Flow	Sample No.	$K_2O^+$ (wt. %)	Extr. No.	Wgt. (gms)	Tracer	Mass Analysis No.	$^{40}Ar/^{38}Ar$		$^{40}Ar$ rad (mol/gm)	$^{40}Ar$ rad (percent)	A Calculated Age ( $10^3$ years)	B Weighted Mean# (10 <sup>3</sup> years)
							$^{38}Ar/^{36}Ar$	$^{38}Ar/^{36}Ar$				
8	76-6-241	0.531 ± 0.002	1	22.535	N	{ A	0.4342	694.6	1.760	3.8	230 ± 85	230 ± 85
						{ B	0.4343	696.0				
9	77-1-299.5	0.459 ± 0.014	1	25.655	N	A	1.814	162.1	3.970	4.8	595 ± 70	230 ± 85
						{ A	0.8680	355.2				
						{ B	0.8678	354.0				
			2	25.422	N	{ A	1.115	271.4	3.185	2.9	480 ± 90	550 ± 60
						{ B	1.115	271.2				
8	BG94-299.5	0.212 ± 0.001	1	26.153	N	{ A	0.7808	382.0	1.333	1.9	435 ± 165	435 ± 165
						{ B	0.7798	382.5				
9	77-1-328.6	0.211 ± 0.020	1	25.465	N	A	0.9123	321.8	<0.8	<1.0	<270	435 ± 165
						{ A	1.101	267.7				
						{ B	1.101	267.4				
			2	25.697	N	{ A	0.6904	428.5	0.7754	1.2	255 ± 190	255 ± 190
						{ B	0.6905	428.6				
12	77-1-569	0.461 ± 0.002	1	22.486	N	{ A	0.8392	360.1	2.852	3.2	430 ± 95	435 ± 75
						{ B	0.8390	360.7				
			2	21.116	N	A	0.7645	396.1	2.959	3.4	445 ± 115	435 ± 75

Argon

Flow	Sample No.	K <sub>2</sub> O <sup>+</sup> (wt. %)	Extr. No.	Wgt. (gms)	Tracer	Mass Analysis No.	40 Ar/38 Ar		38 Ar/36 Ar		40 Ar (mol %)	40 Ar (percent)	A Calculated Age (10 <sup>5</sup> years)	B Weighted Mean (10 <sup>5</sup> years)
							A	B	A	B				
	77-1-572.8	0.216 ± 0.005	1	25.062	N	{ A B }	0.5451 0.5450	546.8 548.5	1.230	2.4	395 ± 180	310 ± 125		
	77-1-594	0.366 ± 0.003	1	25.038	N	{ A B }	0.7025 0.7024	421.4 420.9	0.7184	1.2	230 ± 175			
	77-1-594	0.366 ± 0.003	2	27.324	N	{ A B }	1.022 1.022	294.9 294.8	2.640	2.7	500 ± 130			
	77-1-594	0.366 ± 0.003	2	25.791	N	A	1.292	232.4	2.567	2.2	490 ± 125	495 ± 90		

+ Mean and calculated standard deviation of four measurements.

λ<sub>e</sub> = 0.581 x 10<sup>-10</sup> yr<sup>-1</sup>, λ<sub>β</sub> = 4.962 x 10<sup>-10</sup> yr<sup>-1</sup>, 40K/K = 1.167 x 10<sup>-4</sup> mol/mol. Errors are estimates of the standard deviation of analytical precision (Cox and Dalrymple, 1967).

\* Weighting is by the inverse of the estimated variance.

a Extraction 1 lost because of technical difficulties.

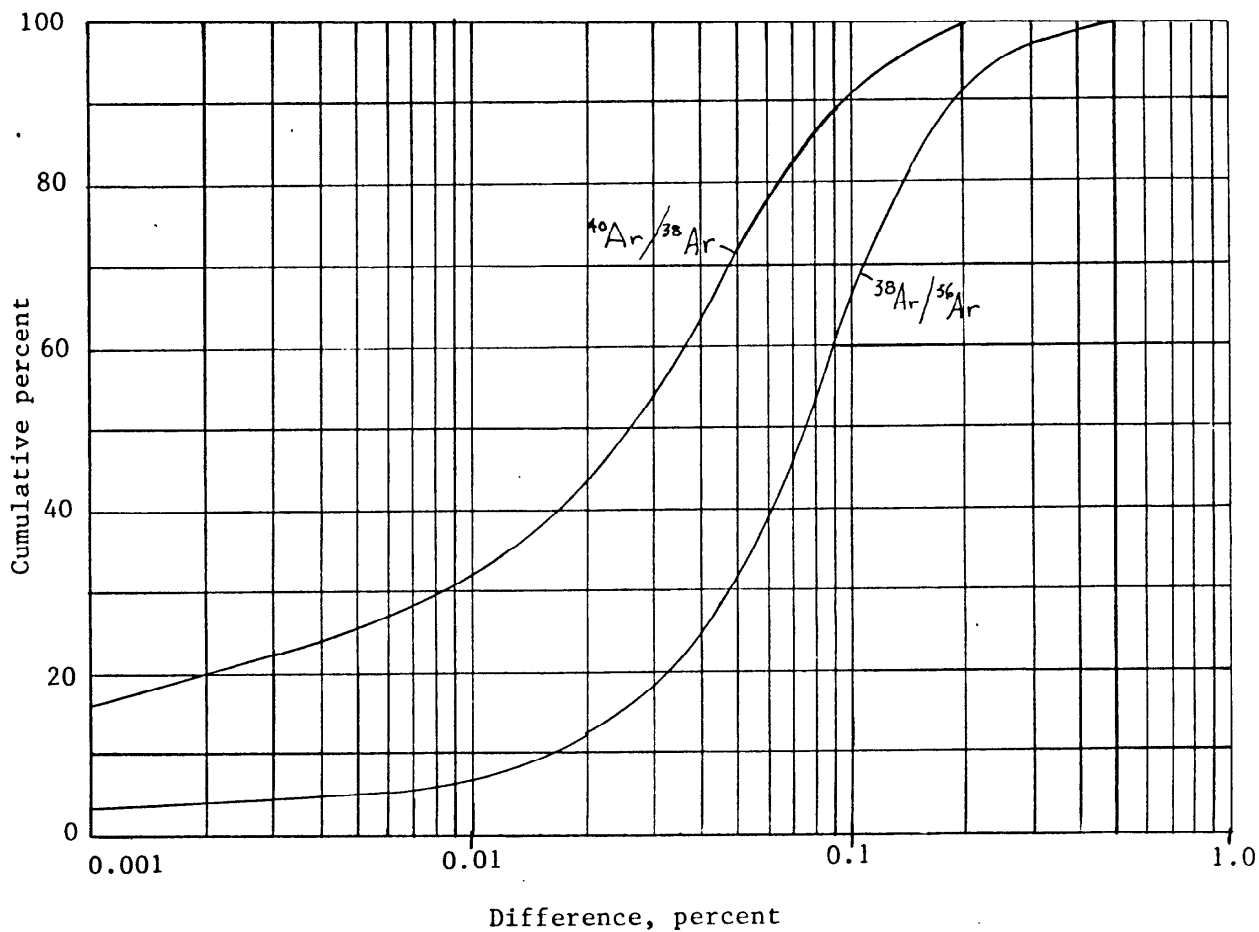


Figure 4.--Cumulative curves showing the difference between replicate mass analyses on the same extraction gas. Class intervals are 0.0015-0.0035, 0.0035-0.0075, 0.0075-0.015, etc.

subtracted from another of similar magnitude (the total  $^{40}\text{Ar}$ ) to find the small remainder (the radiogenic  $^{40}\text{Ar}$ ).

K-Ar ages were calculated from the Ar and  $\text{K}_2\text{O}$  analytical data (table 1) using the new  $^{40}\text{K}$  decay constants ( $\lambda_{\epsilon} + \lambda_{\beta} = 0.581 \times 10^{10} \text{ yr}^{-1}$ ;  $\lambda_{\beta} = 4.962 \times 10^{-10} \text{ yr}^{-1}$ ) recommended by the IUGS Subcommittee on Geochronology (Steiger and Jager, 1977). Errors given in table 2 are estimates of the standard deviation of precision on the individual calculated age and were estimated using the method of Cox and Dalrymple (1967). Ages were not calculated for samples with radiogenic  $^{40}\text{Ar}$  contents of less than one percent. Instead a maximum age was calculated and represents what the calculated age would be if there were one percent radiogenic  $^{40}\text{Ar}$  in the analysis.

#### Results

Because the lava flows are both geologically very young and low in  $\text{K}_2\text{O}$ , the fraction of radiogenic  $^{40}\text{Ar}$  in the sample gas is small; it ranges from 0 to a maximum of only 4.8 percent. As a result, the estimated uncertainties in the calculated ages of individual samples are large. The uncertainties range from 12 percent (77-1-299.5(1)) to 76 percent (77-1-572.8(2)). The reason is that the theoretical error in a K-Ar age increases rapidly as the percentage of radiogenic  $^{40}\text{Ar}$  decreases below about 10 percent (fig. 5). The error calculations are also very sensitive to the estimates of the errors in the individual quantities measured. For example, for a sample with two percent radiogenic  $^{40}\text{Ar}$ , an increase in the estimated error of the  $^{38}\text{Ar}/^{36}\text{Ar}$  ratio from 0.5 to 1.0 percent nearly doubles the theoretical error in the calculated age. Finally, the error calculations do not take into account geological factors, such as sample inhomogeneity, that frequently result in errors even

Table 2. Mean ages of lava flows for data in Table 1.

Flow	Mean Age ( $10^3$ years)			Probability of difference
	1	2	3	
1	95 ± 50	95 ± 50	95 ± 50	--
2	<200	<200	<200	--
3	<190	<190	<190	>99
5	290 ± 5	290 ± 45	290 ± 45	--
6	180 ± 15	180 ± 0	180 ± 30	96
7	205 ± 45	205 ± 40	210 ± 25	88
8	230 ± 84	230 ± 84	230 ± 84	42
9	440 ± 140	415 ± 150	515 ± 85	18
12	375 ± 100	375 ± 90	400 ± 75	98
13	495 ± 5	495 ± 90	495 ± 90	69

- 1 - Simple mean and standard deviation of calculated ages in Column A, Table 1.
- 2 - Simple mean and standard deviation of calculated ages in Column B, Table 1.
- 3 - Weighted mean of calculated ages in Column B, Table 1, with estimated standard deviations of precision.

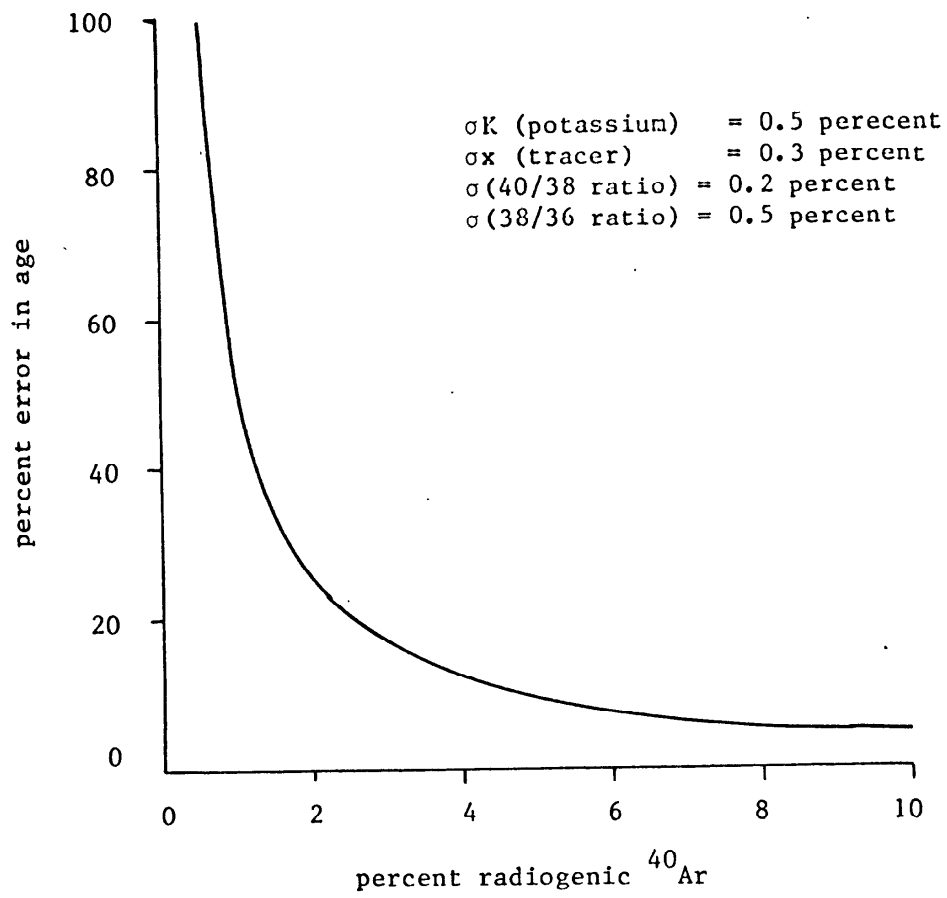


Figure 5.--Theoretical error curve for K-Ar ages as a function of the percentage of radiogenic  $^{40}\text{Ar}$  in the sample gas. Based on the error formula of Cox and Dalrymple (1967).

larger than those in the measurements. Because of these factors, errors assigned to the calculated ages are only estimates of analytical precision for single samples, and the data should be treated accordingly.

Statistical analysis of the data shows that there is no significant difference between the calculated ages of individual runs (extr. nos. 1 and 2, table 1) on the same sample, or between the calculated ages of different samples from the same flow at the 95-percent level of confidence.

The K-Ar age data for each lava flow have been averaged in several ways, as summarized in table 2. Column 1 of table 2 gives the simple means and calculated standard deviations of all of the calculated ages for each flow in column A of table 1. Column 2 of table 2 gives the means and standard deviations of the data in column B of table 1. Neither of these methods takes into account the estimated errors in analytical precision for each calculated age, so a poor (low radiogenic  $^{40}\text{Ar}$ ) analysis is given the same weight as a better (higher radiogenic  $^{40}\text{Ar}$ ) analysis. Column 3 of table 2 contains the weighted means, where weighting is by the inverse of the variance of the mean ages for each sample (column B, table 1). This technique takes into account the estimated analytical uncertainties of the individual measurements as well as the number of measurements made on each sample. The mean ages in column 3 of table 2 are probably the least biased and are the best estimates of the K-Ar ages of the flows.

The probability that a real difference in apparent K-Ar age has been detected has been calculated for all possible pairs of flow mean ages and those data are shown in table 2 as the "probability of difference" in percent. These probabilities are based on the mean ages and errors in column 3 of table 2. As the errors are estimates, the probabilities are only semiquantitative.

With only two exceptions, the flow mean ages (column 3, table 2) agree with the known stratigraphic relationships in the drill holes. The calculated age of flow 5 appears to be greater than that of flow 6 (but not flows 7 or 8) at the 95-percent confidence level. This age is based on data from a single sample (77-1-126) for which the duplicate analyses agree well. The other apparent anomaly is flow 9, which appears older than flows 12, and 13, but the difference is not significant at the 95-percent confidence level.

#### PALEOMAGNETISM

##### Analytical techniques

Mini-core specimens were taken from three of the five drill cores to determine the polarity and inclination of remanent magnetization at various depths. It was anticipated that this information could be used to determine boundaries of significant time separation between lava flows. As none of the original drill cores were oriented with regard to azimuth, it was not possible to determine the magnetic declination. Each lava flow identified by macroscopic and petrographic work, as well as any additional unit noted during paleomagnetic sampling, was sampled for the magnetic studies. Nominally, seven mini-core samples were taken from each unit, but fewer samples were taken from some units because the material was insufficient. Multiple sampling was required because a volcanic rock only imperfectly records the local magnetic field vector at the time of cooling, and measurement of multiple samples tends to average out inaccuracies. The possibility that samples of the drill core had been turned upside down during previous handling was taken into consideration, but the paleomagnetic studies showed that prior handling of the core was careful and that none of the cores had been inverted.

Specimens for magnetic analysis were obtained with a 2.5 cm-diameter core drill at right angles to the axis of the original core. Assuming that the original cores were vertical, we drilled all specimens on randomly oriented horizontal axes. The core specimens were trimmed with a cut-off saw to 2.2-cm lengths, and orientation marks recording the vertical plane through each specimen were put on the specimens.

All specimens were measured with a spinner magnetometer (Doell and Cox, 1967). Volcanic rocks typically acquire a large thermoremanent magnetization (TRM) at the time they cool, thus their TRM is generally easy to measure. All specimens were initially measured to determine the direction of their natural remanent magnetization (NRM). Two specimens from each lava flow were then chosen for stepwise demagnetization experiments in an alternating field demagnetizer to determine the field strength required to remove all components of secondary magnetization acquired since acquisition of their original TRM (Doell and Cox, 1976). Typically, the principal secondary magnetization is a viscous remanent magnetization (VRM) acquired by thermal unlocking of magnetic domains by the Earth's field through time. Additionally, a lightning strike close to a specimen would impart a strong isothermal remanent magnetization (IRM) to the rock. The stepwise alternating field demagnetization experiments indicated what peak field strengths were sufficient to "clean" each specimen from each lava flow. The field strengths were usually 20 mT\* for those units with normal polarity and, because of slightly larger VRM effects, 30 mT for units having reversed polarity. After cleaning, only one specimen was discarded for spurious inclination information; all other specimens gave reasonable groupings for each lava flow.

\* mT = milli-Tesla (units are kg/sec/coulomb)

## Results

The magnetic inclination and polarity information make it possible to subdivide the original cores on the basis of their stratigraphy and remanent magnetic direction. This analysis necessarily assumes a model of the long term behavior of the magnetic field at the site of the drill cores. For this study, the model assumed is one of virtually constant motion of the magnetic field vector with time. This model can be justified from other work which documents values of  $4^{\circ}$  to  $5^{\circ}$  of angular motion per century (Champion and Shoemaker, 1977). These values are means, as the angular motion has occasionally been as much as  $10^{\circ}$  or as little as  $0^{\circ}$  per century. This model of the magnetic field allows an interpretation of the amount of time represented by a boundary between two lava flows. With the additional information that basalt eruptions of the Snake River Plain tend to be episodic, short-lived, and voluminous (Kuntz, 1978b), the time separation likely represents thousands or tens of thousands of years (Champion and Shoemaker, 1977).

The remanent magnetic results obtained in this study are shown in figure 6. The boundaries identified in the macroscopic and petrographic work are shown on the figure with solid lines. Additional physical boundaries identified during paleomagnetic studies by zones of high vesicularity, oxidation, and brecciation are shown as dashed lines. Solid circles denote normal polarity inclinations and open circles denote reversed polarity. The data reveal that the remanent magnetization within individual flows is all of the same magnetic polarity. This uniformity shows that the drill cores have been handled carefully since the original coring and that core slugs have not been randomly turned upside down. For each flow, a mean inclination and a

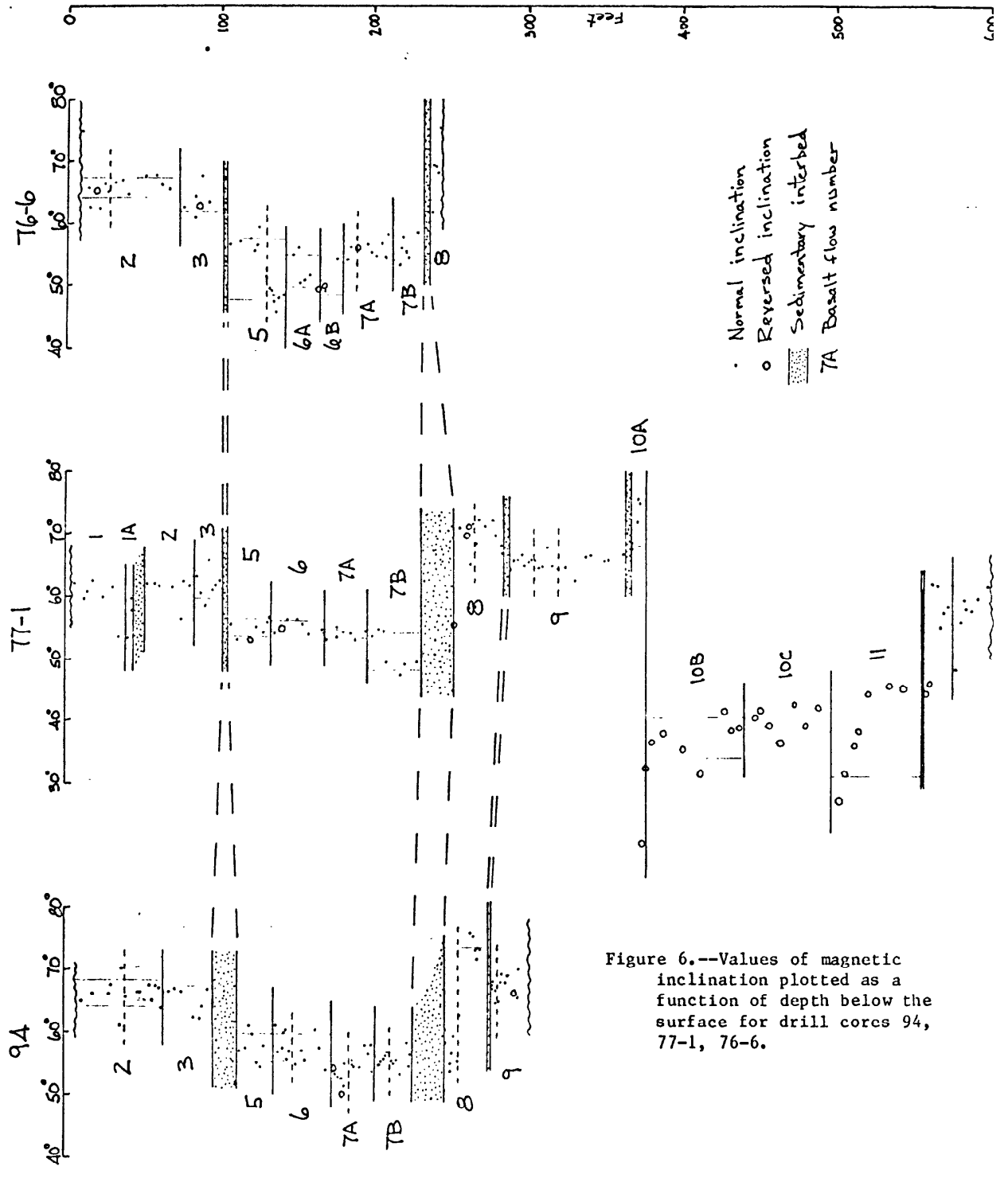


Figure 6.--Values of magnetic inclination plotted as a function of depth below the surface for drill cores 94, 77-1, 76-6.

standard deviation have been calculated (table 3), and they are shown on figure 5 as shaded fields enclosing the area within one standard deviation of the mean.

Only core 77-1 penetrates to depths below approximately 91 m at the RWMC site. This is unfortunate because lava flows below that depth have interesting remanent magnetic characteristics. Flows 12 and 13 are clearly separated by a flow break, but they show nearly identical inclination values. Assuming the model described above, this relationship suggests that flows 12 and 13 are flow units of two eruptive episodes that are separated by less than 100 years.

Flows 10B, 10C, and 11 have reversed magnetic polarity and have inclinations that are shallower than the inclinations of other flows. The sedimentary interbed between flow 11 and flow 12 thus represents a period of time necessary to produce a reversal of the magnetic field. Estimates of the time required to produce a reversal vary, with typical values ranging from 1,000 to 10,000 years (Irving, 1964; McElhinny and Merrill, 1975). The top two samples from flow 12, at 170.1 m and 170.7 m, are also reversed in polarity and have the same inclinations as samples in the overlying lava of flow 11. This reversal is likely due to a thermal remagnetization of the upper part of flow 12 at the time flow 11 was erupted. Basalt has relatively low thermal conductivity; thus, heating did not appreciably affect a sample at 171.6 m. The depth of local heating in flow 12 is, therefore, between 1 and 2 meters.

Flow 11 has somewhat dispersed inclinations, a progressive change of inclination upward, and one of the largest standard deviations of any lava flow studied. This dispersion may be due to tilting of the upper portions of

Table 3. Mean Magnetic inclination values with one standard deviations for lava flows in 3 cores from RWMC, INEL, Idaho.

Group	Flow Number	Drill core Number		
		94	77-1	76-6
A	1	- - -	$60.0^{\circ} \pm 3.1^{\circ}$	- - -
	1A	- - -	$56.9^{\circ} \pm 3.2^{\circ}$	- - -
B	2	$66.1^{\circ} \pm 2.1^{\circ}$	$61.1^{\circ} \pm 2.0^{\circ}$	$65.6^{\circ} \pm 1.6^{\circ*+}$
	3	$65.1^{\circ} \pm 2.1^{\circ}$	$61.9^{\circ} \pm 2.3^{\circ}$	$64.0^{\circ} \pm 2.2^{\circ*}$
C	5	$57.6^{\circ} \pm 2.3^{\circ}$	$54.9^{\circ} \pm 1.4^{\circ*}$	$52.4^{\circ} \pm 4.9^{\circ}$
	6A	$57.6^{\circ} \pm 2.2^{\circ+}$	$55.2^{\circ} \pm 1.0^{\circ*}$	$52.3^{\circ} \pm 2.6^{\circ*}$
	6B			$51.2^{\circ} \pm 2.7^{\circ*}$
	7A	$54.5^{\circ} \pm 2.2^{\circ*}$	$54.0^{\circ} \pm 0.8^{\circ}$	$55.6^{\circ} \pm 1.4^{\circ*}$
	7B	$55.7^{\circ} \pm 1.2^{\circ}$	$51.2^{\circ} \pm 3.0^{\circ}$	$55.9^{\circ} \pm 1.9^{\circ}$
D	8	$64.8^{\circ} \pm 8.6^{\circ}$	$69.9^{\circ} \pm 2.1^{\circ*+}$	$68.8^{\circ} \pm 4.9^{\circ}$
E	9	$67.5^{\circ} \pm 1.6^{\circ*}$	$65.5^{\circ} \pm 1.1^{\circ}$	- - -
F	10A	- - -	$71.7^{\circ} \pm 3.6^{\circ+}$	- - -
	10B	- - -	$-37.2^{\circ} \pm 3.2^{\circ}$	- - -
	10C	- - -	$-40.1^{\circ} \pm 2.1^{\circ}$	- - -
	11	- - -	$-38.2^{\circ} \pm 7.2^{\circ}$	- - -
G	12	- - -	$58.5^{\circ} \pm 3.0^{\circ+}$	- - -
	13	- - -	$56.8^{\circ} \pm 4.3^{\circ}$	- - -

\* Specimen(s) with spurious polarity was(were) interverted for inclusion in this inclination mean.

+ Specimen(s) was(were) omitted from this mean inclination.

- - - No data

the flow after some TRM had been acquired within the upper 6 m. If one discards the inclinations from flow 11 that are assumed to have been affected by deformation, there is a progressive change of  $8^{\circ}$  of inclination evident up through flow 10B. The progressive change of inclination probably indicates a span of time less than or equal to 200 years, if we use the nominal rate of angular change for the magnetic field vector ( $4^{\circ}/100$  yr), and if we assume that all field motion took place as inclination change and none as declination change. These data then suggest that flows 11, 10C, and 10B were emplaced within a period of approximately 200 years.

Flow 10A shows some reversed inclinations but mostly normal, steep inclinations. These inclinations could be an indication of an error in the position of the stratigraphic boundaries, but, by analogy with flow 12, it seems more likely that flow 10A has been magnetically overprinted by flow 9. Owing to the low thermal conductivity of basalt, this overprint extends only 9 feet into the upper part of flow 10A. Thus, despite the normal inclinations at the top, flow 10A is reversed in polarity and belongs to eruption group F.

Flow 9 was penetrated in drill cores 94 and 77-1. In drill core 77-1, samples throughout flow 9 have virtually identical inclinations that suggest that flow 9 is a single flow. What appear to be minor flow breaks are thus recognized as zones of differential flowage, as described in the previous section on the petrography of flow 9. Flow 9 is overlain by a thin (0.3 m) sedimentary interbed, which separates it from flow 8, which has inclinations that are  $6^{\circ}$  steeper than the inclinations of flow 9. This sedimentary interbed probably represents an interval of no less than 150 years. Flow 8 in drill core 76-6 has inclinations that become progressively shallower upward. The progressive shallowing of the inclinations suggests possible thermal

remagnetization by the overlying flow. In drill core 77-1, there is a similar change in inclination. However, flow 8 is overlain at a depth of 73 m by a sedimentary interbed 1.2 m to 9.8 m thick, and remagnetization by the overlying flow therefore is unlikely. In drill core 94, division of flow 8 into upper and lower units is indicated by different inclinations. The top 9 feet of the flow may have been deformed by as much as  $15^{\circ}$  relative to the stably magnetized bottom, which has inclinations near  $72^{\circ}$ . In drill core 77-1 the mean inclination for flow 8 is about  $70^{\circ}$ . In drill core 76-6, thermal remagnetization may have affected the top sample of flow 8, but the lower samples have a mean inclination value in the high 60's. The simplest and most likely interpretation of these relations is that flow 8 represents a single outpouring of lava that encompasses less than 100 years.

The best interpretation of the magnetic data for flows 5, 6A, 6B, 7A, and 7B is that group C represents flows from an eruption(s) that occurred over a short period of time. This interpretation is principally derived from the inclination data in drill core 77-1. Flows 5 through the top of 7A all show inclinations in the mid 50's. The inclinations for the bottom of flow 7B are in the high 40's. In drill core 94, the inclinations of flows 5 through the top of 7A are slightly higher, probably because of a slight difference in the magnetic backgrounds between drill cores 77-1 and 94, but the inclinations are similar through the sequence. In drill core 76-6, the bottom flows, 7A and 7B, and the upper part of flow 5 also record inclinations in the mid 50's. Flows 6A and 6B and the lower part of flow 5, on the other hand, all show lower inclinations. The lower inclinations for Flows 6A, 6B, and 5 in drill core 76-6 could represent valid records of the local magnetic field, but when compared with inclinations for the same flows in other holes, they probably

represent moderate amounts of tilting of these flows after the acquisition of TRM. In summary, the remanent magnetic data for flows of group C suggest emplacement of a sequence of thin flow units within a century of time, accompanied by minor amounts of tilting. The difference in inclination values across the 73-m (240-ft) sedimentary interbed indicates that 400 years or more separate the flows of group C from the single flow of group D.

The entire sequence of flows in groups A and B shows similar mean inclinations in drill cores 94, 77-1, and 76-6. Comparison reveals slight differences in the mean inclinations of flows among the 3 drill cores. These differences are probably due to local magnetic anomaly differences among the three drill cores. There may be large time differences between flows, but the inclination data suggests that the amount of time between flows is small, probably on the order of a few tens of years. The sediment interbed at 15.2 m in drill core 77-1 may represent a considerable amount of time between the emplacement of flows 2 and 1A, although a flood could possibly have deposited the sediment layer in a short period of time during this eruptive sequence. The difference in inclinations across the 33.5-m sediment interbed suggests that the flows of groups B and C are separated by 200 years or more.

#### AGE AND FREQUENCY OF ERUPTION OF LAVA FLOWS

The stratigraphic, petrographic, radiometric, and paleomagnetic data show that a minimum of 18 lava flows and flow units (fig. 3) have inundated the area in and adjacent to the RWMC in the last 500,000 years. The individual lava flows and flow units are arranged in seven groups of flows, consisting of from one to five flows and flow units. The average rate of inundation of the RWMC site is thus approximately one group of flows per 70,000 years. It is clear, however, that the eruptions were episodic rather than periodic. Each

inundation event probably lasted less than 200 years, and the events were separated by long intervals of time during which no lava flows entered the area. The estimated ages and durations of these volcanic events and the lengths of the intervening periods of quiescence are summarized in table 4.

The eruption of the lava flows may be divided into at least three major eruption episodes on the basis of their K-Ar ages (table 2). The inclinations also aid in determining the time represented by a sequence of flows. Previous studies of secular variation have shown that the inclination of the field changes about  $4^{\circ}$ - $5^{\circ}$  per century, although the change is not necessarily regular (Champion and Shoemaker, 1977). The lack of detectable change in inclination between successive flows suggests, therefore, that they were erupted within a period of less than 100 years.

The oldest eruption episode is represented by lava of groups E, F, and G. The K-Ar ages of the four lava flows dated in this group are not significantly different at the 95 percent level of confidence, and the data are consistent with an age for all flows of approximately  $450,000 \pm 50,000$  years. The paleomagnetic and petrographic data show that this set of flow units consists of three groups. The paleomagnetic and petrographic data indicate that group E consists of a single flow (flow 9) and, as such, it was emplaced within a very short period of time, probably no more than a few days or weeks. This flow has normal polarity. Flows 10 and 11 (group F) have reversed polarity and show a small but consistent change in inclination from about  $40^{\circ}$ - $45^{\circ}$  to  $35^{\circ}$ - $40^{\circ}$ . This change in inclination indicates that the eruption of these flows may have occurred over a period of time of as much as 200 years. Based on the lack of change in magnetic inclination, we estimate that flows 12 and 13 (group G) were erupted within a period of less than 100 years.

Table 4.--Summary of lava flow frequency represented in drill cores from the Radioactive Waste Management Complex, Idaho National Engineering Laboratory, Idaho.

Groups	Flows	Age(yr)	Time Interval(yr)	Minimum # of flows	Thickness (meters) (from 77-1)
A & B	1-3	50,000-100,000	<100	3	31
***** Major Time Break (100,000-200,000 yrs)*****					
C	5-7	225,000	<100	4	38
----- Minor Time Break (400 yrs-100,000 yrs) -----					
D	8	225,000	<100	1-2	10
***** Major Time Break (100,000-250,000 yrs)*****					
E	9	450,000	<100	2	23
----- Minor Time Break (1,000-100,000 yrs) -----					
F	10-11	450,000	<200	3-4	57
----- Minor Time Break (1,000-100,000 yrs) -----					
G	12-13	450,000	<100	2	13

The K-Ar data suggest that the time intervals between flows of groups E, F and G were probably less than 100,000 years; otherwise, a significant age difference would have been detected. The magnetic inclinations show that sufficient time passed between the emplacement of the flows of groups E and F for the Earth's field to completely reverse its polarity without the lava flows recording the transition. The time required for a polarity reversal is not known exactly, but it has been estimated to be of the order of 1,000 to 10,000 years (Irving, 1964; McElhinny and Merrill, 1975). Thus, the minimum time between the emplacement of the three groups was probably about 1,000 years.

The next eruption episode is represented by flows 5-8. The K-Ar data indicate that these flows are about  $225,000 \pm 25,000$  years old. The paleomagnetic, stratigraphic, and petrographic data indicate that these flows were erupted in two groups. The oldest (group D) consists of lava flow 8, the youngest (group C) consists of lava flows 5-7. The paleomagnetic inclinations indicate that the lava flows of group C were emplaced within a period of less than 100 years. Flow 8 probably represents a single event in spite of the difference in inclinations from hole 94, as explained in the discussion of the paleomagnetic results. The K-Ar data indicate that the time interval between eruption of groups C and D was less than 100,000 years. The difference in magnetic inclinations between the two groups indicates that the minimum time interval between their formation was at least 400 years, but the thickness and lateral extent of the sediment interbed between the groups suggest that the period may have been thousands or tens of thousands of years, rather than hundreds of years.

The youngest eruption episode consists of flows 1-4, which were erupted in groups A and B. Only flow 1 yielded a definite K-Ar age of  $95,000 \pm 50,000$  years, which is consistent with a carbon-14 age of greater than 40,000 years on charcoal found beneath this flow. The consistency of the paleomagnetic inclinations suggests that the lava flows of groups A and B could have been emplaced within a period of less than 100 years. The radiometric data are consistent with an age of approximately  $75,000 \pm 25,000$  for groups A and B.

#### APPLICATION OF DATA TO EVALUATION OF VOLCANIC

#### HAZARDS AT THE RADIOACTIVE WASTE MANAGEMENT COMPLEX

A previous study by Kuntz (1978b) noted that the chief volcanic hazard for the RWMC was inundation by lava flows erupted from both distant and nearby source vents. These vents and the RWMC both lie within a topographic basin. It is assumed that local igneous activity has not yet died out, thus future source vents within the boundaries of the topographic basin all have the potential of delivering lava flows to the RWMC site. Kuntz identified 47 volcanic vents less than about 200,000 years old within the basin, but the stratigraphic and radiometric data presented here show that only a fraction of the lavas erupted from those vents actually reached the RWMC site.

Our interpretation of the stratigraphy (table 1), and along with age information (figure 3), suggests that at least 11 lava flows and flow units, erupted from 4 or more source vents, have inundated the RWMC area within about the last 225,000 years. Thus, the data suggest that eruptions from roughly 1 in 5 vents within the basin have produced enough lava to reach the RWMC area.

Any future eruption within the basin poses a potential hazard to the RWMC, but our data suggest that only about 20 percent of such eruptions would

actually inundate the RWMC. The likelihood of inundations will increase for any single, future eruption if that eruption (1) is from a source vent near the RWMC, (2) lasts a relatively long time and produces voluminous amounts of lava, and (3) is of the lava-cone or shield eruption variety.

Should the RWMC be inundated by lava, the principal effect on the surficial and buried waste would be localized heating. Theoretical calculations of the degree of heating beneath a lava flow assume that conduction would be the form of heat dissipation, that emplacement of the flow would be instantaneous, and that thermal properties of all materials would be uniform (Lovering, 1935). Lovering's calculations indicate that temperatures of 350<sup>o</sup>-400<sup>o</sup>C would be reached at depths of 3.3 to 4.6 m beneath flow 9, assuming an initial temperature difference of 1100<sup>o</sup>C, and that these temperatures would be reached 2 to 3 years after the emplacement of the lava flow. Using the paleomagnetic data from this study, it is possible to determine the actual level of heating beneath flow 9 in hole 77-1 and check the theoretical calculations. Thermal demagnetization of a specimen from flow 10 at a depth of 114 m in hole 77-1 shows that the specimen was heated to 350<sup>o</sup> to 400<sup>o</sup>C by the overlying flow 9, even though separated by 1 m of alluvium and 2.4 m of overlying basalt. Thus the single empirical check from this study indicates that simple theoretical calculations may provide realistic estimates of the temperatures reached in the buried waste as a result of inundation of the site by lava.

Other types of volcanic hazards for the RWMC are described in Kuntz (1978b).

#### ACKNOWLEDGMENTS

We thank James Saburomaru for sample preparation, S. E. Simms, B. M. Myers, and J. C. VonEssen, for argon analyses, and P. R. Klock for potassium measurements. Gordon Thrupp assisted with the paleomagnetic measurements and computation. J. D. Obradovich, of the U.S.G.S. in Denver, Colorado, generously provided us with the use of his mass spectrometric facilities while our Menlo Park instruments were undergoing unanticipated repairs. Jack Barraclough of the U.S.G.S. at the INEL provided support and advice for obtaining core samples.

#### REFERENCES CITED

- Barraclough, J. T., Robertson, J. B., and Janzer, V. J., 1976, Hydrology of the solid waste burial ground as related to the potential migration of radionuclides, Idaho National Engineering Laboratory, with a section on drilling and sample analyses by L. G. Saindon: U.S. Geological Survey Open-File Report 76-471, 183 p.
- Burgus, W. H., and Maestas, S. E., 1976, The 1975 RWMC core drilling program, a further investigation of subsurface radioactivity at the Radioactive Waste Management Complex, Idaho National Engineering Laboratory: U.S. Energy Research and Development Administration, Idaho Operations Office, Report IDO-10065, 36 p.
- Champion, D. E., and Shoemaker, E. M., 1977, Paleomagnetic evidence for episodic volcanism on the Snake River Plain. (abs.): NASA Technical Memorandum 78,436, p. 7-9.
- Cox, A., and Dalrymple, G. B., 1967, Statistical analysis of geomagnetic reversal data and the precision of potassium-argon dating: *Journal of Geophysical Research*, v. 72, p. 2603-2614.
- Dalrymple, G. B., and Lanphere, M. A., 1969, Potassium-argon dating: San Francisco, W. H. Freeman and Co., 258 p.
- Doell, R. R., and Cox, A. V., 1967, Analysis of spinner magnetometer operation, in *Methods in paleomagnetism*, Collinson, D. W., Creer, K. M., and Runcorn, S. K. eds: Elsevier Publishing Co., Amsterdam, p. 196-206.
- Doell, R. R., and Cox, A. V., 1976, Analysis of alternating field demagnetization equipment, in *Methods in paleomagnetism*, Collinson, D. W., Creer, K. M., and Runcorn, S. K., eds: Elsevier Publishing Co., Amsterdam, p. 214-253.

- Fountain, J. C., and Spear, D. B., 1979, Geochemistry of ferrobasalt, ferrolatite, and rhyolite lavas from the Cedar Butte area, eastern Snake River Plain, Idaho (abstr.): Geological Society of America Abstracts with Programs, v. 11, no. 6, p. 272-273.
- Garner, E. L., Murphy, T. J., Gramlich, J. W., Paulsen, P. J., and Barnes, I. L., 1975, Absolute isotopic abundance ratios and the atomic weight of a reference sample of potassium: Journal of Research, National Bureau of Standards--A. Phys. and Chem., v. 79A, p. 713-725.
- Humphrey, T. G., and Tingey, F. H., 1978, The subsurface migration of radionuclides at the Radioactive Waste Management Complex: U.S. Department of Energy, Idaho Operations Office, Report TREE-1171, 98 p.
- Ingamells, C. O., 1970, Lithium metaborate flux in silicate analysis: Anal. Chimica. Acta., v. 52, p. 323-334.
- Irving, E., 1964, Paleomagnetism: New York, John Wiley and Sons, Inc., 399 p.
- Kuntz, Mel A., 1978a, Geologic map of the Arco Big Southern Butte area, Butte, Blaine, and Bingham Counties, Idaho: U.S. Geological Survey Open-File Report 78-302.
- Kuntz, Mel A., 1978b, Geology of the Arco-Big Southern Butte area, eastern Snake River Plain, and potential volcanic hazards to the Radioactive Waste Management Complex and other waste storage and reactor facilities at the Idaho National Engineering Laboratory, Idaho, with a section on Statistical treatment of the age of lava flows by John O. Kork: U.S. Geological Survey Open-File Report 78-691, 70 p.

- Lanphere, M. A., and Dalrymple, G. B., 1976, Final compilation of K-Ar and Rb-Sr measurements of P-207, the U.S. Geological Survey interlaboratory standard muscovite: U.S. Geological Survey Professional Paper 840, p. 127-130.
- Lovering, T. S., 1935, Theory of heat conduction applied to geological problems: Geological Society of America Bulletin, v. 46, p. 69-94.
- Mankinen, E. A., and Dalrymple, G. B., 1972, Electron microprobe evaluation of terrestrial basalts for whole-rock dating: Earth and Planetary Science Letters, v. 17, p. 89-94.
- McElhinny, M. W., and Merrill, R. T., 1975, Geomagnetic secular variation over the past 5 m.y.: Reviews of Geophysics and Space Physics, v. 13, no. 5, p. 687-708.
- Steiger, R. N., and Jager, E., 1977, Subcommittee on geochronology: Convention on the use of decay constants in geo- and cosmochemistry: Earth and Planetary Science Letters, v. 36, p. 359-362.